Possibilities to Identify Cavity due to UNE Using Seismic Wave Fields

Jozef KRISTEK [1,2] Miriam KRISTEKOVA [2,1] Peter MOCZO [1,2]

Peter LABAK [3] Martin GALIS [1,2]

[1]Comenius University Bratislava

[2]Earth Science Institute Slovak Academy of Sciences

[3]CTBTO

Motivation

In collaboration with the CTBT Organisation

to investigate possibilities

of the resonance seismometry

for on-site inspection (OSI)

using

3D modelling of seismic wave fields

in realistic models of the underground structure

after an underground nuclear explosion (UNE) set of structural models based on the in-depth literature survey

cavity without chimney (for plastic rock)

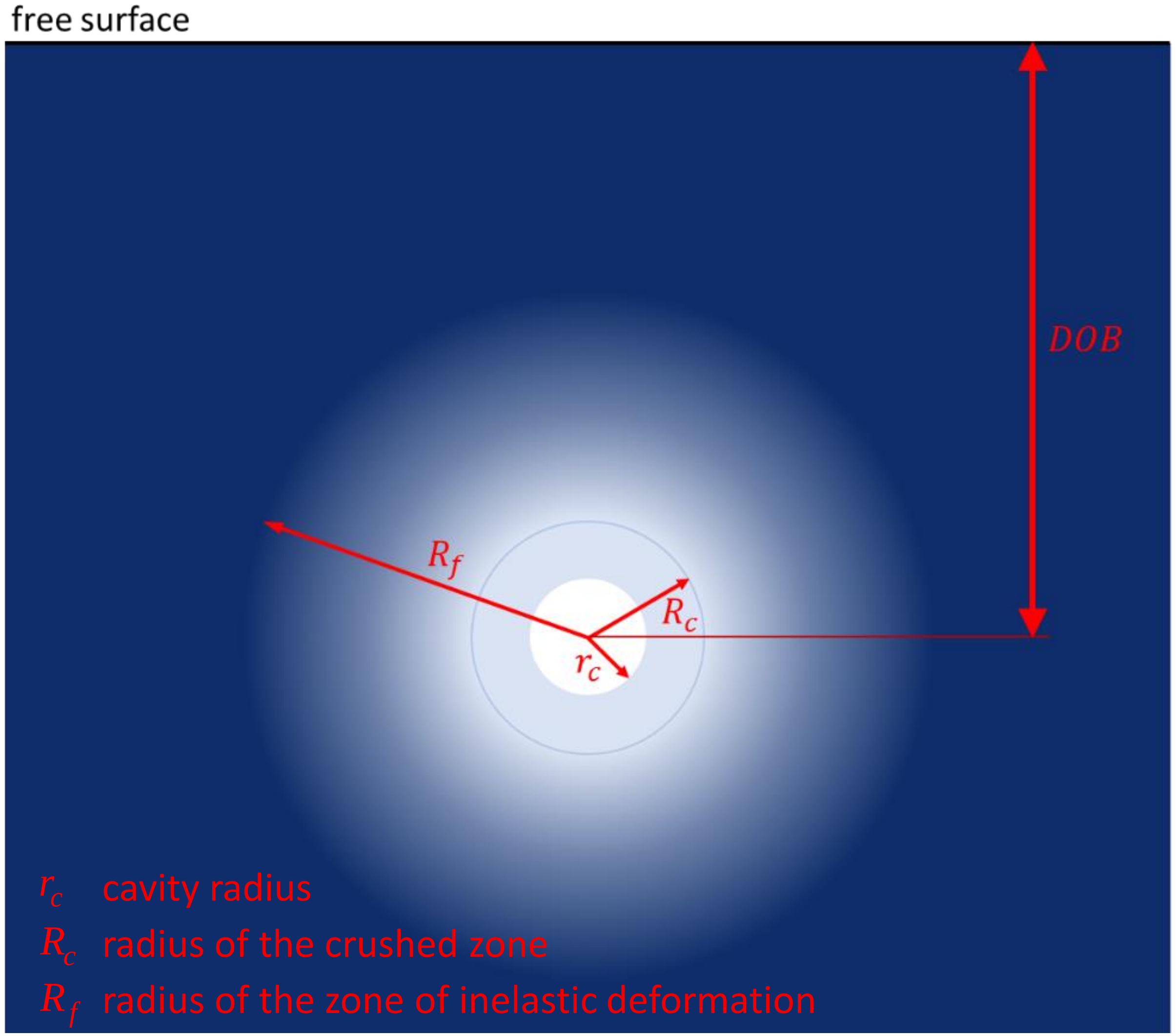

cavity with chimney filled with rubble + apical void

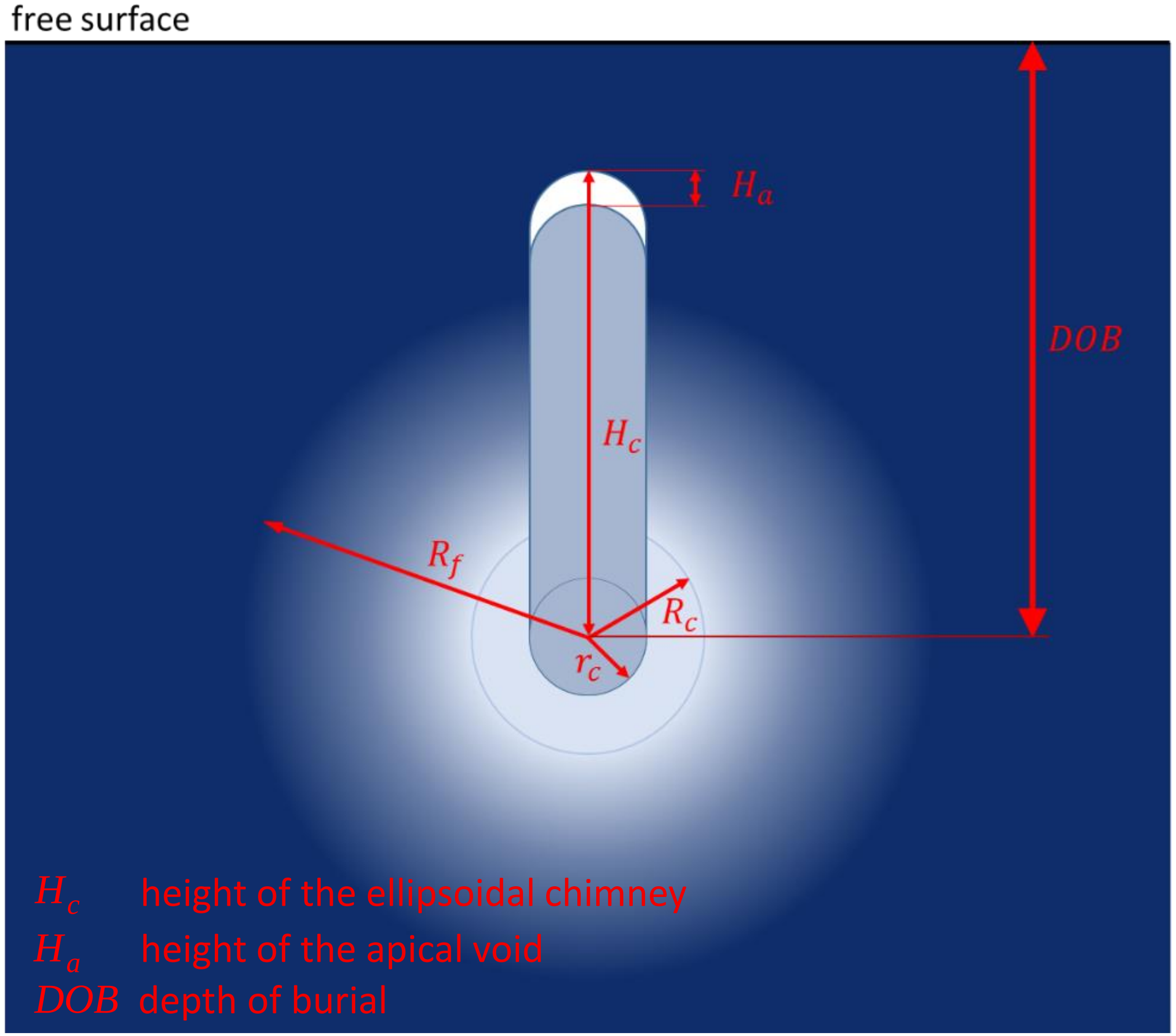

set of structural models based on the in-depth literature survey

4 essential types of preshot media

- tuff
- alluvium
- rock salt
- granite

with **viscoelastic attenuation**

$$Q_S(f) = \frac{V_S}{10}$$

$$Q_\kappa(f) = \infty$$

3 different fillings of cavity/apical void

fluid (high Vp)
gas (low Vp)
vacuum

2 different yields of explosion

low-yield (1 kt)
high-yield (10 kt)

2 different depth of burial

minimal
2 x minimal

in total: **48 basic structural models**

material	yield	depth of burial	r_c	R_c	R_f	H_c	H_a
tuff	low	180	16.9 ± 0.8	25.4 ± 1.1	67.5 ± 3.0	138 ± 20	9.7 ± 1.4
		360	15.6 ± 1.8	23.4 ± 2.7	56.4 ± 6.5	127 ± 18	8.9 ± 1.3
	high	280	33.4 ± 2.6	50.2 ± 3.9	125.9 ± 9.8	256 ± 16	18.0 ± 1.1
		560	30.9 ± 5.2	46.4 ± 7.8	102 ± 17	237 ± 15	16.6 ± 1.0
alluvium	low	180	14.6 ± 2.2	22.0 ± 3.3	118 ± 18	120 ± 17	8.4 ± 1.2
		360	13.4 ± 1.5	20.1 ± 2.3	88.1 ± 9.9	109 ± 15	7.6 ± 1.1
	high	260	29.0 ± 2.6	43.5 ± 3.8	212 ± 19	222 ± 14	15.6 ± 1.0
		520	26.5 ± 1.4	39.8 ± 2.1	153.6 ± 8.1	204 ± 12	14.2 ± 0.9
granite	low	180	11.5 ± 2.4	22.9 ± 4.8	196 ± 41	75 ± 12	5.2 ± 0.8
		360	10.5 ± 2.1	21.0 ± 4.2	142 ± 28	62 ± 18	4.4 ± 1.3
	high	260	22.7 ± 3.2	45.3 ± 6.5	344 ± 49	173 ± 25	12.1 ± 1.8
		520	20.8 ± 3.0	41.6 ± 6.0	242 ± 35	143.2 ± 8.0	10.0 ± 0.6
rock salt	low	180	14.8 ± 0.9	22.2 ± 1.4	188 ± 12	-	-
		360	13.7 ± 1.7	20.5 ± 2.5	130 ± 16	-	-
	high	260	29.5 ± 2.0	44.3 ± 3.0	323 ± 22	-	-
		520	27.3 ± 4.3	40.9 ± 6.4	219 ± 34	-	-

3D numerical simulations

- numerical simulations using 3D finite-difference modeling code
  - (4,2) heterogeneous finite-difference scheme on staggered grid
  - internationally verified code FDSim (www.nuquake.eu/fdsim)
  - a novel approach to simulate vacuum cavities

3D numerical simulations

- numerical simulations using 3D finite-difference modeling code
  - (4,2) heterogeneous finite-difference scheme on staggered grid
  - internationally verified code FDSim (www.nuquake.eu/fdsim)
  - a novel approach to simulate vacuum cavities
- verification
  - vacuum cavity in a homogeneous halfspace
  - fluid-filled cavity in a homogeneous unbounded medium

3D numerical simulations

- numerical simulations using 3D finite-difference modeling code
  - (4,2) heterogeneous finite-difference scheme on staggered grid
  - internationally verified code FDSim (www.nuquake.eu/fdsim)
  - a novel approach to simulate vacuum cavities

- verification
  - **vacuum cavity in a homogeneous halfspace**
  - fluid-filled cavity in a homogeneous unbounded medium

vacuum cavity in a homogeneous halfspace

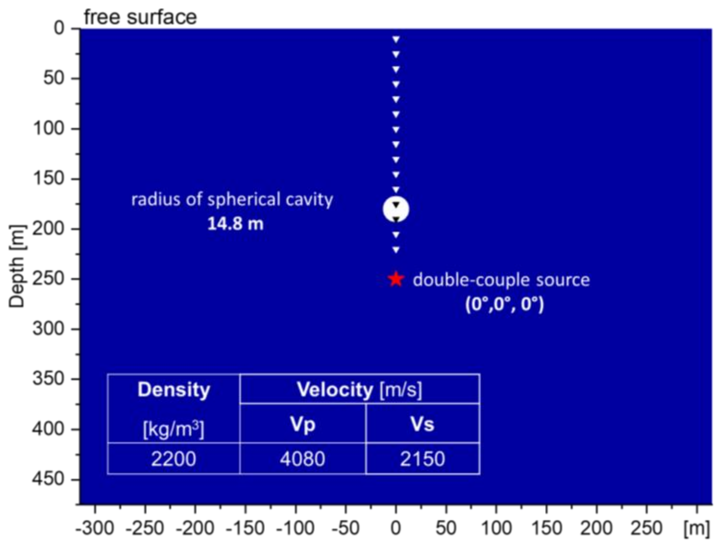

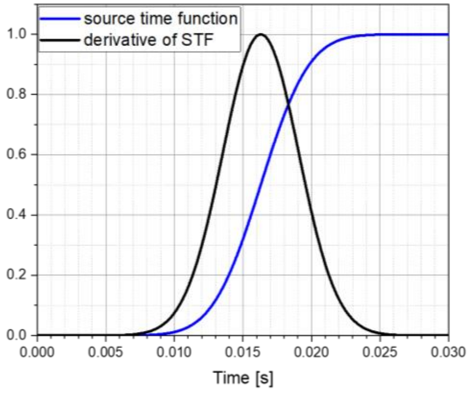

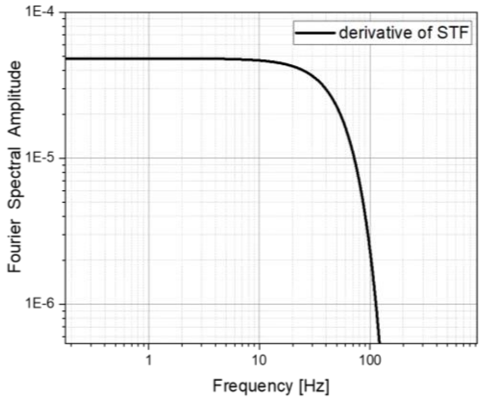

Horizontal component of particle velocity
(seismograms and snapshots)

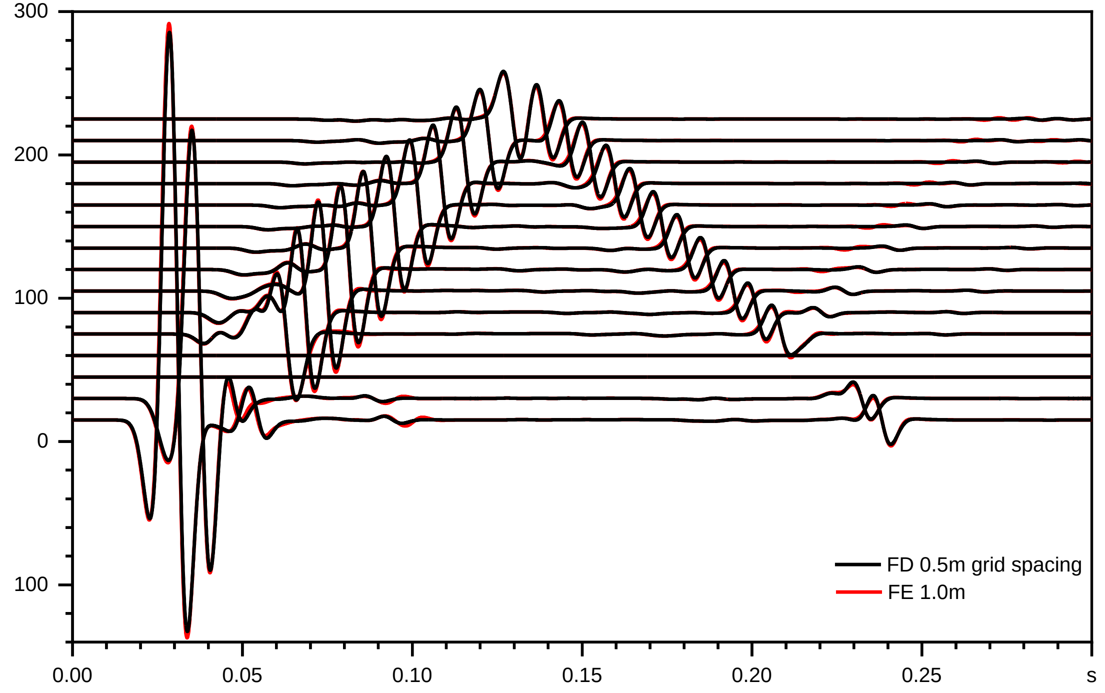

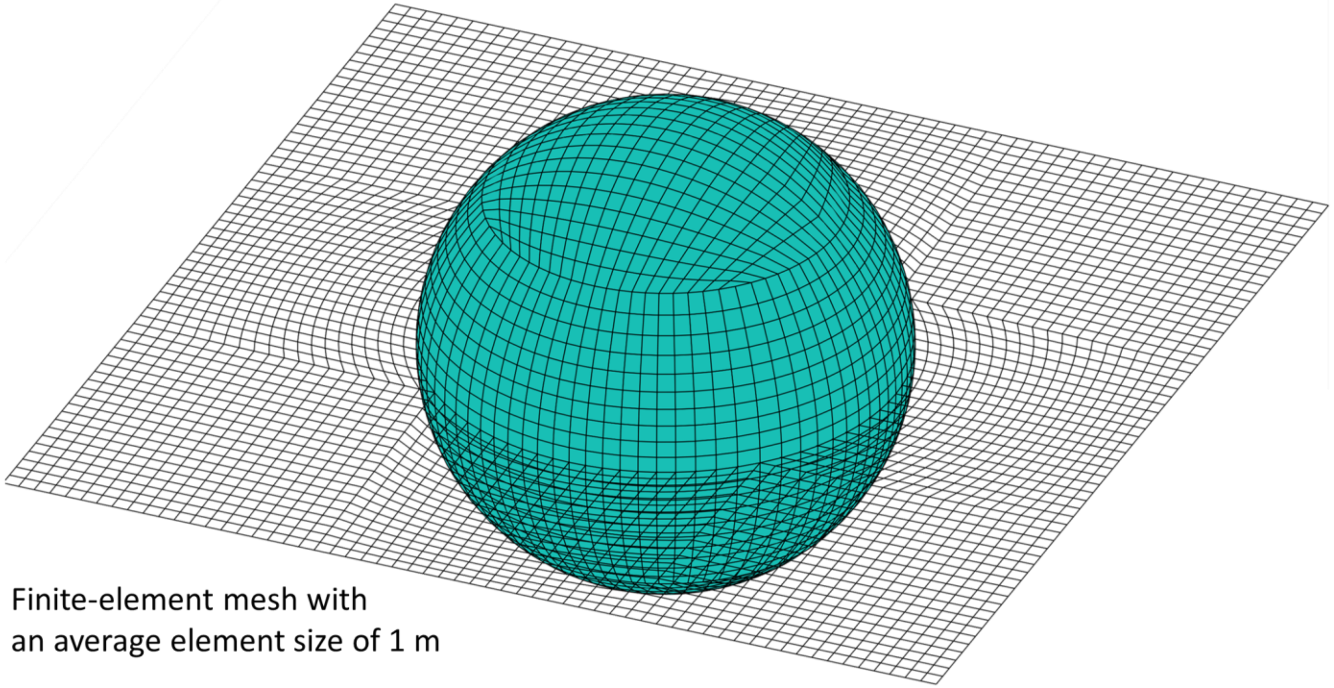

Finite-element mesh with
an average element size of 1 m

vacuum cavity in a homogeneous halfspace

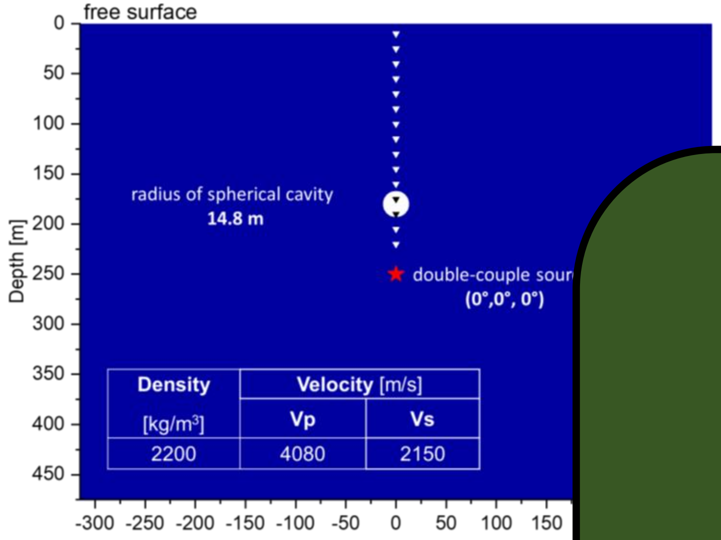

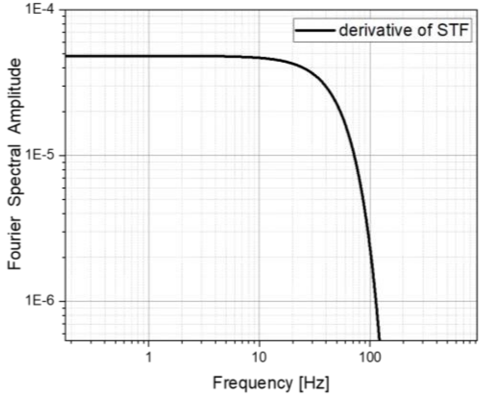

All FD-FE comparisons
lead to conclusion
that our FD modeling
is well applicable
to numerical modeling
of seismic wave propagation
in media with vacuum cavities

Horizontal compon
(seismogram

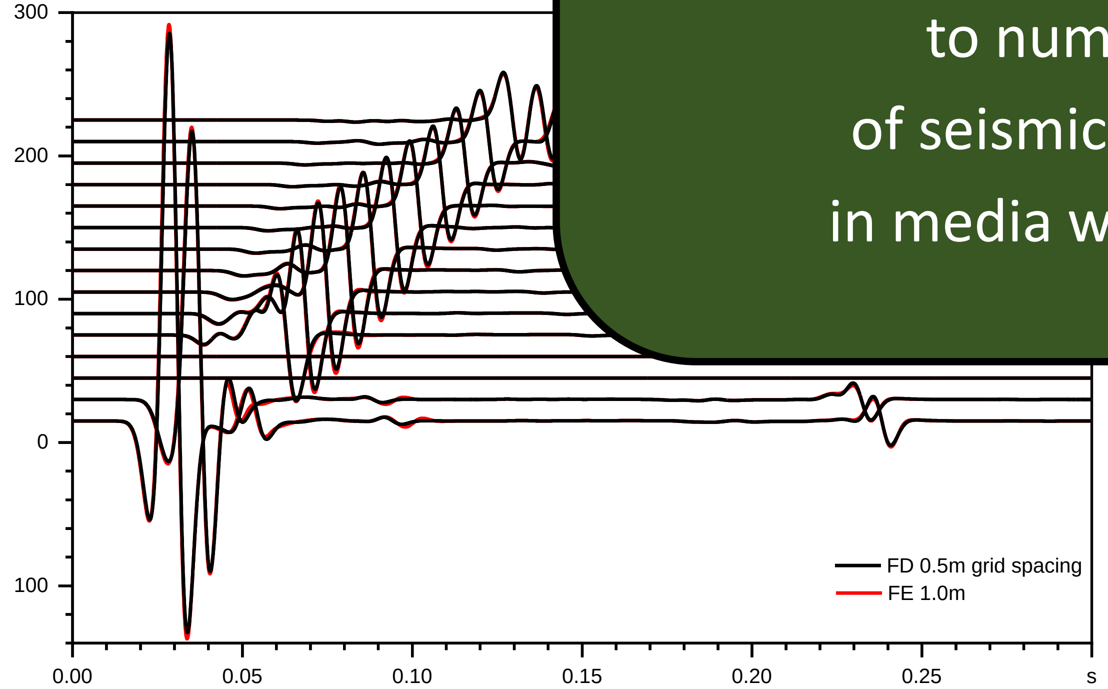

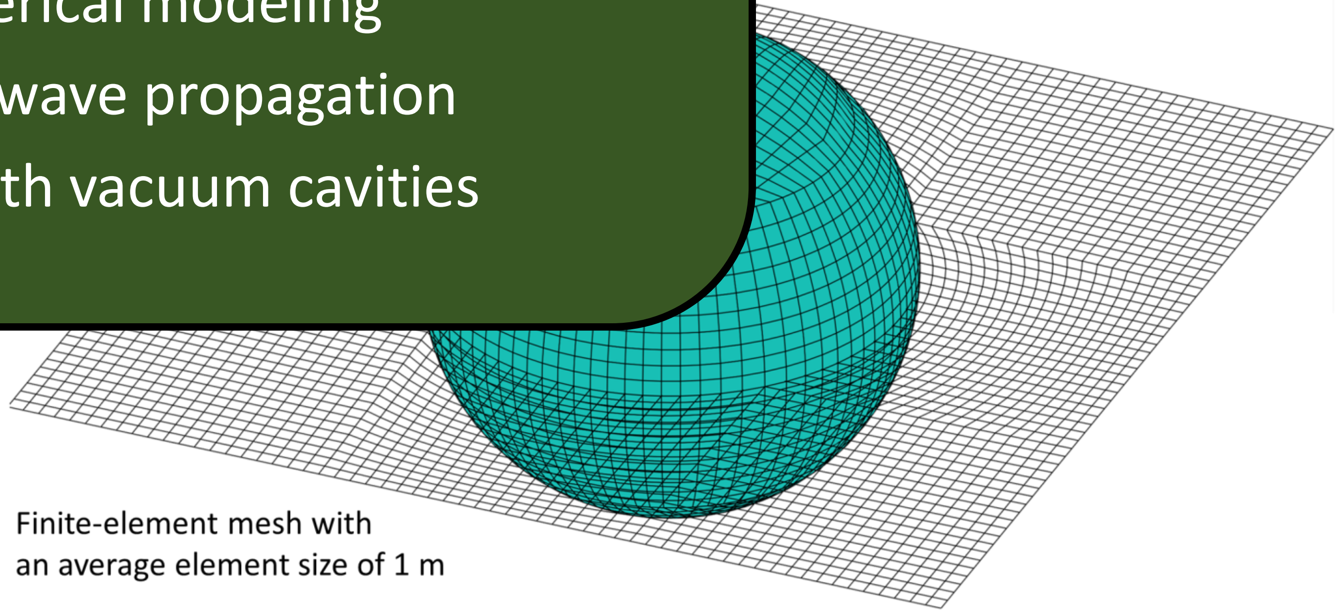

Finite-element mesh with
an average element size of 1 m

3D numerical simulations

- numerical simulations using 3D finite-difference modeling code
  - (4,2) heterogeneous finite-difference scheme on staggered grid
  - internationally verified code FDSim (www.nuquake.eu/fdsim)
  - a novel approach to simulate vacuum cavities
- verification
  - vacuum cavity in a homogeneous halfspace
  - **fluid-filled cavity in a homogeneous unbounded medium**

fluid-filled cavity in a homogeneous unbounded medium

The vertical component of the particle velocity simulated by
DG-SEM (Sofi Esterhazy, code Speed; blue)
and our FDM (black)
at 2 selected profiles of receivers

Domain	Vp [m/s]	Vs [m/s]	Density [kg/m^3]
Outside	4000	2310	2700
Inside	1500	0	1000

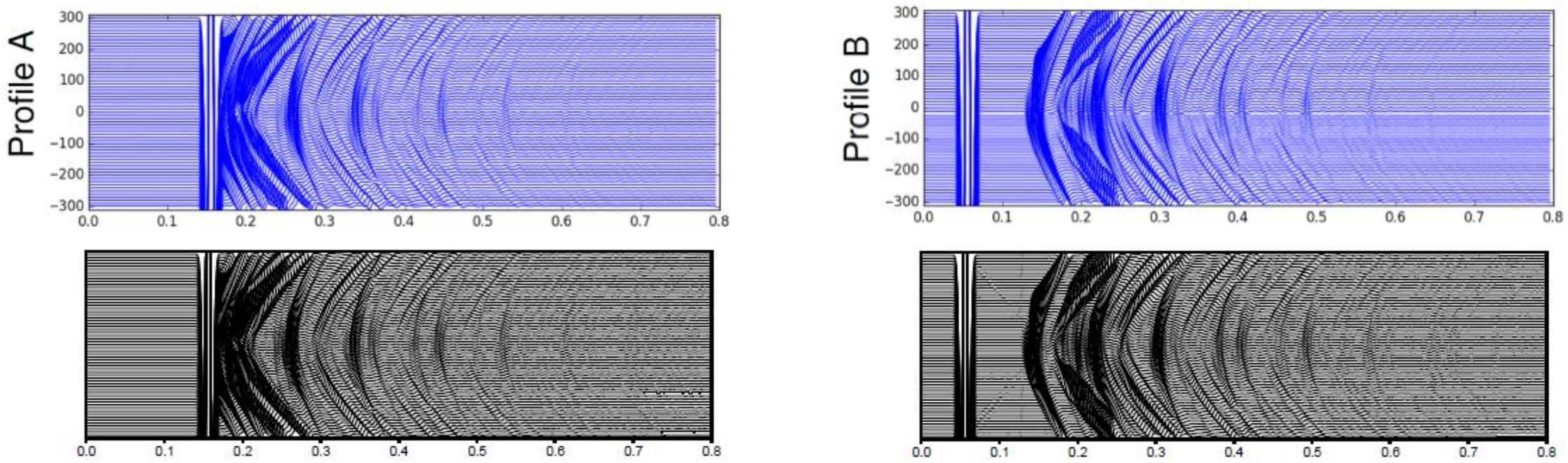

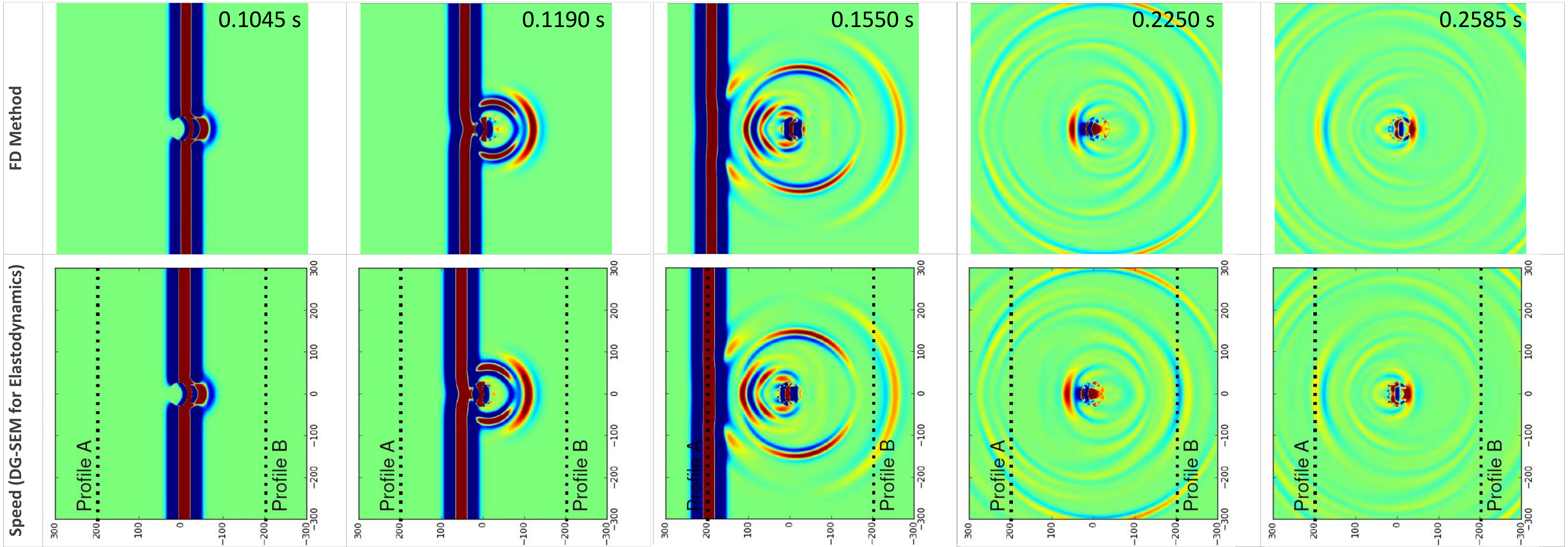

fluid-filled cavity in a homogeneous unbounded medium

The vertical component of the particle velocity simulated by DG-SEM (Sofi Esterhazy, code Speed; blue) and our FDM (black) at 2 selected profiles of receive

Domain	Vp [m/s]	Vs [m/s]	Den [kg/
Outside	4000	2310	27
Inside	1500	0	10

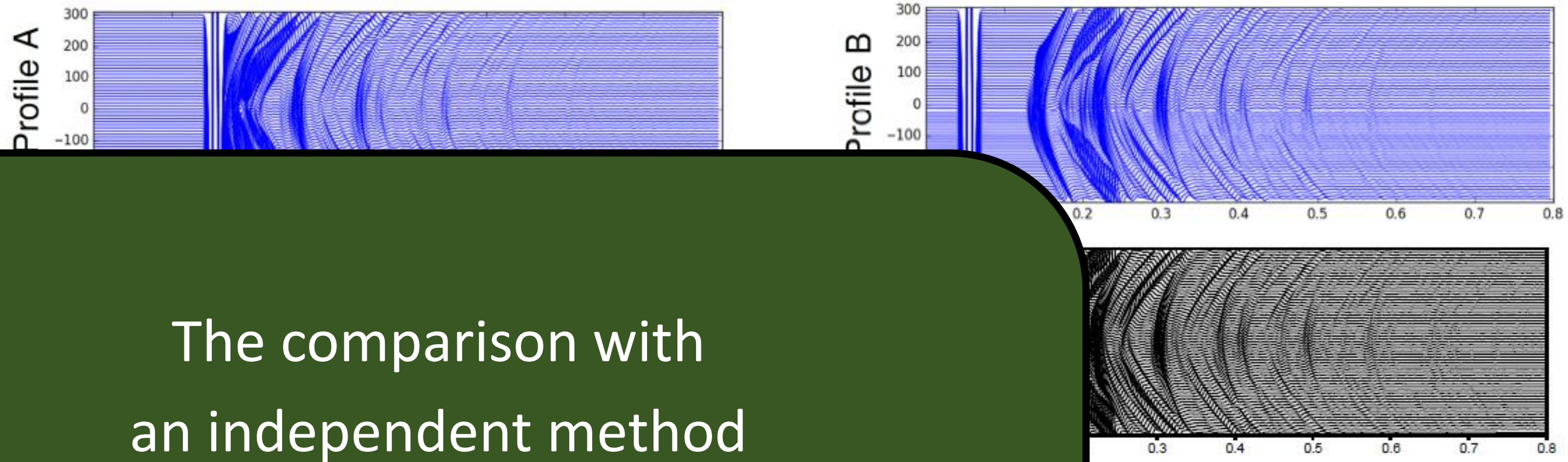

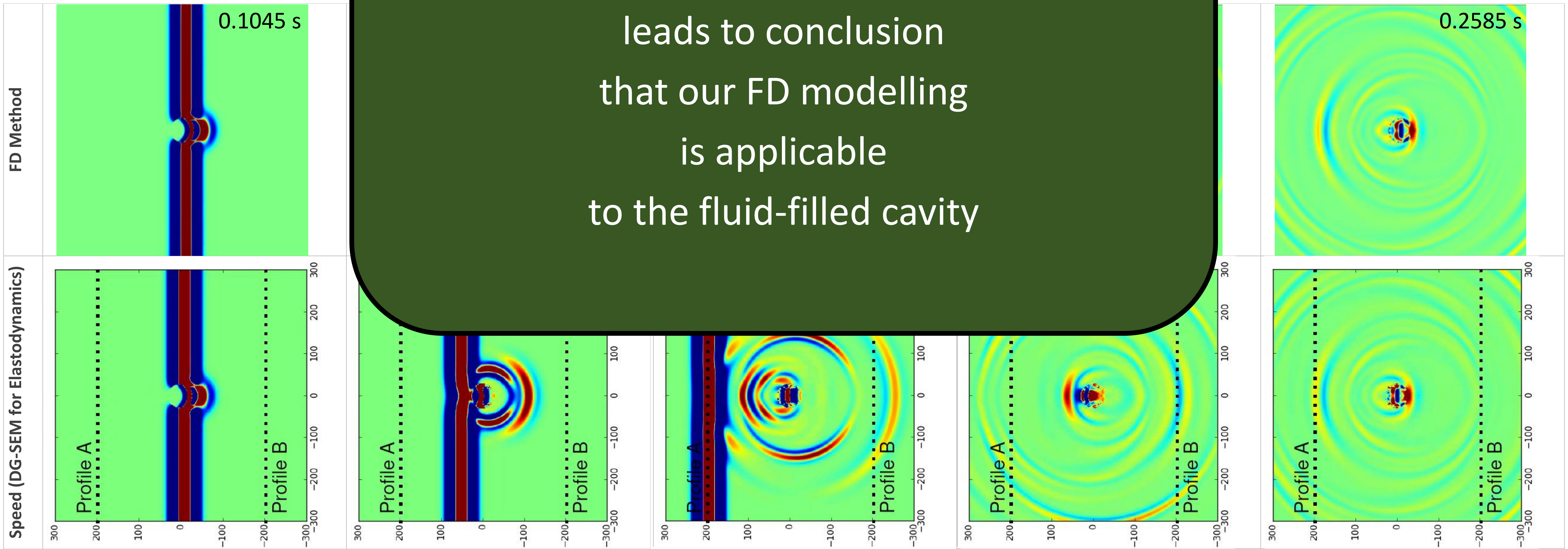

The comparison with
an independent method
leads to conclusion
that our FD modelling
is applicable
to the fluid-filled cavity

3D numerical simulations

- wavefield excitation
    - three types of plane wave:
        - one P-wave
        - two S-waves with orthogonal polarities
    - point source representing an aftershock
    - ambient noise
- number of receivers in one simulation: 6400
- frequency range up to 20 Hz
- time window at least 30 s

3D numerical simulations

- wavefield excitation
  - **three types of plane wave**:
    - one P-wave
    - two S-waves with orthogonal polarities
  - point source representing an aftershock
  - ambient noise
- number of receivers in one simulation: 6400
- frequency range up to 20 Hz
- time window at least 30 s

3D numerical simulations

- wavefield excitation
  - **three types of plane wave**:
    - one P-wave
    - two S-waves with orthogonal polarities
    - hock
    - 00
  - frequency range up to 20 Hz
- time window at least 30 s

These types of excitation enable
to compute matrix
of the Fourier transfer functions
of the medium

3D numerical simulations

- wavefield excitation
    - three types of plane wave:

      one P-wave

      two S-waves with orthogonal polarities
    - **point source representing an aftershock**
    - ambient noise
- number of receivers in one simulation: 6400
- frequency range up to 20 Hz
- time window at least 30 s

3D numerical simulations

- wavefield excitation
  - three types of plane wave:
    - one P-wave
    - two S-waves with orthogonal polarities
  - **point source representing an aftershock**

For assumed yields, aftershocks will have magnitudes -1.

We also assume random distribution
of parameters of focal mechanism
(strike, dip and rake).

3D numerical simulations

- wavefield excitation
  - three types of plane wave:
    - one P-wave
    - two S-waves with orthogonal polarities
  - point source representing an aftershock
  - **ambient noise**
- number of receivers in one simulation: 6400
- frequency range up to 20 Hz
- time window at least 30 s

3D numerical simulations

modeling of ambient seismic noise

sources of ambient seismic noise

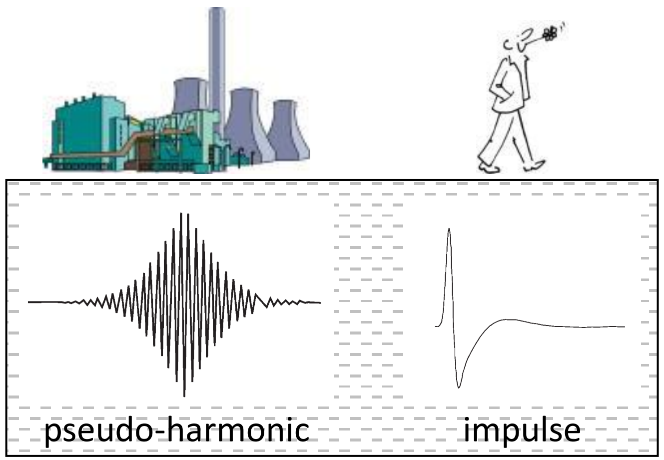

for this study we used only impulse (delta-like) sources

example of randomly generated point sources (body forces)

time functions

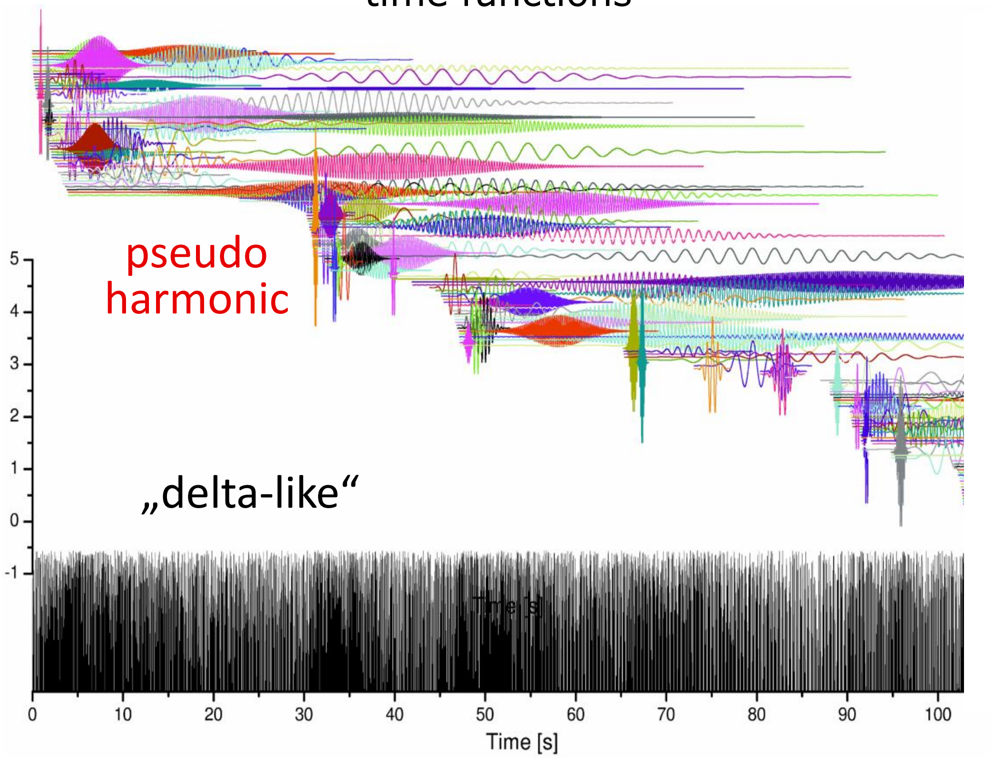

space-time distribution

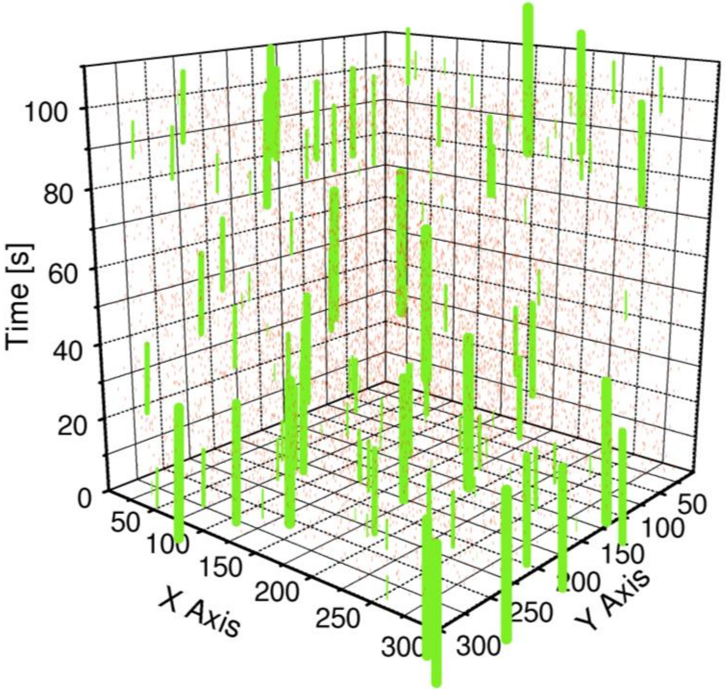

3D numerical simulations

- wavefield excitation
  - three types of plane wave:
    - one P-wave
    - two S-waves with orthogonal polarities
  - point source representing an aftershock
  - ambient noise
- **number of receivers in one simulation: 6400**
- frequency range up to 20 Hz
- time window at least 30 s

3D numerical simulations

- wavefield excitation

uniform dense grid of receivers
at the free surface
covering area
of 800m x 800m
with interstation distance of 10m
centered around the cavity
projected on the free surface

onal polarities

shock

- **number of receivers in one simulation: 6400**
- frequency range up to 20 Hz
- time window at least 30 s

3D numerical simulations

- wavefield excitation
  - three types of plane wave:
    - one P-wave
    - two S-waves with orthogonal polarities
  - point source representing an aftershock
  - ambient noise
- number of receivers in one simulation: 6400
- **frequency range up to 20 Hz**
- time window at least 30 s

3D numerical simulations

- wavefield excitation
    - three types of plane wave:
        - one P-wave
        - two S-waves with orthogonal polarities
    - point source representing an aftershock
    - ambient noise
- number of receivers in one simulation: 6400
- frequency range up to 20 Hz
- **time window at least 30 s**

Results of analysis

- the effects of cavity/apical-void filling
- the effects of attenuation
- analysis of seismic wavefields due to regional and distant seismic sources
- analysis of seismic wavefields due to weak local aftershocks
- analysis of simulated ambient noise

Results of analysis

- **the effects of cavity/apical-void filling**
- the effects of attenuation
- analysis of seismic wavefields due to regional and distant seismic sources
- analysis of seismic wavefields due to weak local aftershocks
- analysis of simulated ambient noise

The effects of cavity/apical-void filling

Select

Medium

- ○ tuff (model with chimney)
- ◉ rock salt

Component

- ◉ horizontal EW

Receiver position (-200,0) m

[center of cavity is at (0, 0) m]

Type of excitation

plane S-wave (EW)

Low yield (1kt)

Minimal depth of burial (180m)

elastic model

Comparison of the effect of **different types of filling** of the cavity on time-frequency representations of seismograms

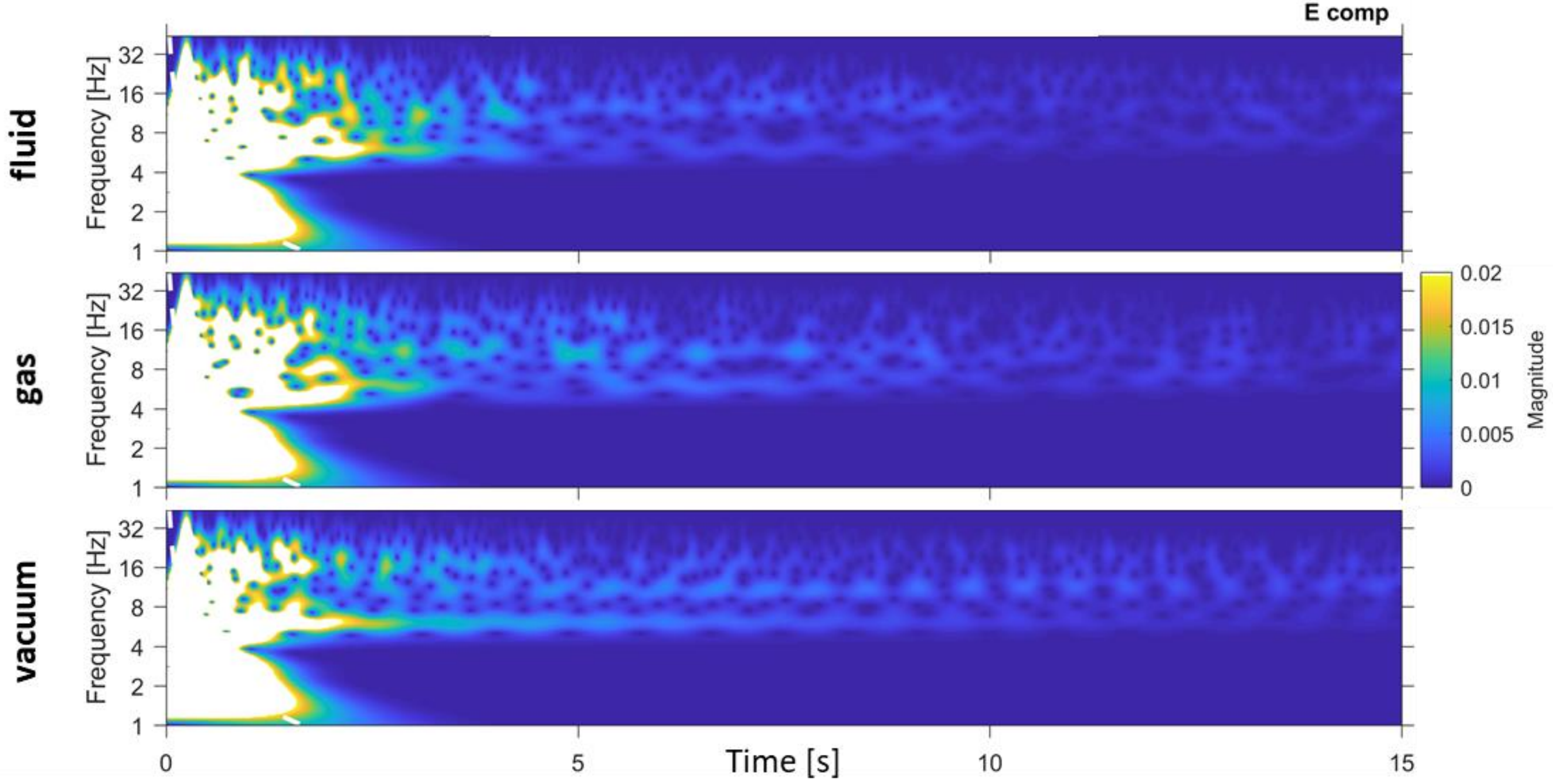

The effects of cavity/apical-void filling

Select

Medium

◉ tuff (model with chimney)

○ rock salt

Component

◉ horizontal EW

Receiver position (-200,0) m

[center of cavity is at (0, 0) m]

Type of excitation

plane S-wave (EW)

Low yield (1kt)

Minimal depth of burial (180m)

elastic model

Comparison of the effect
of **different types of filling**
of the apical void on
time-frequency representations of seismograms

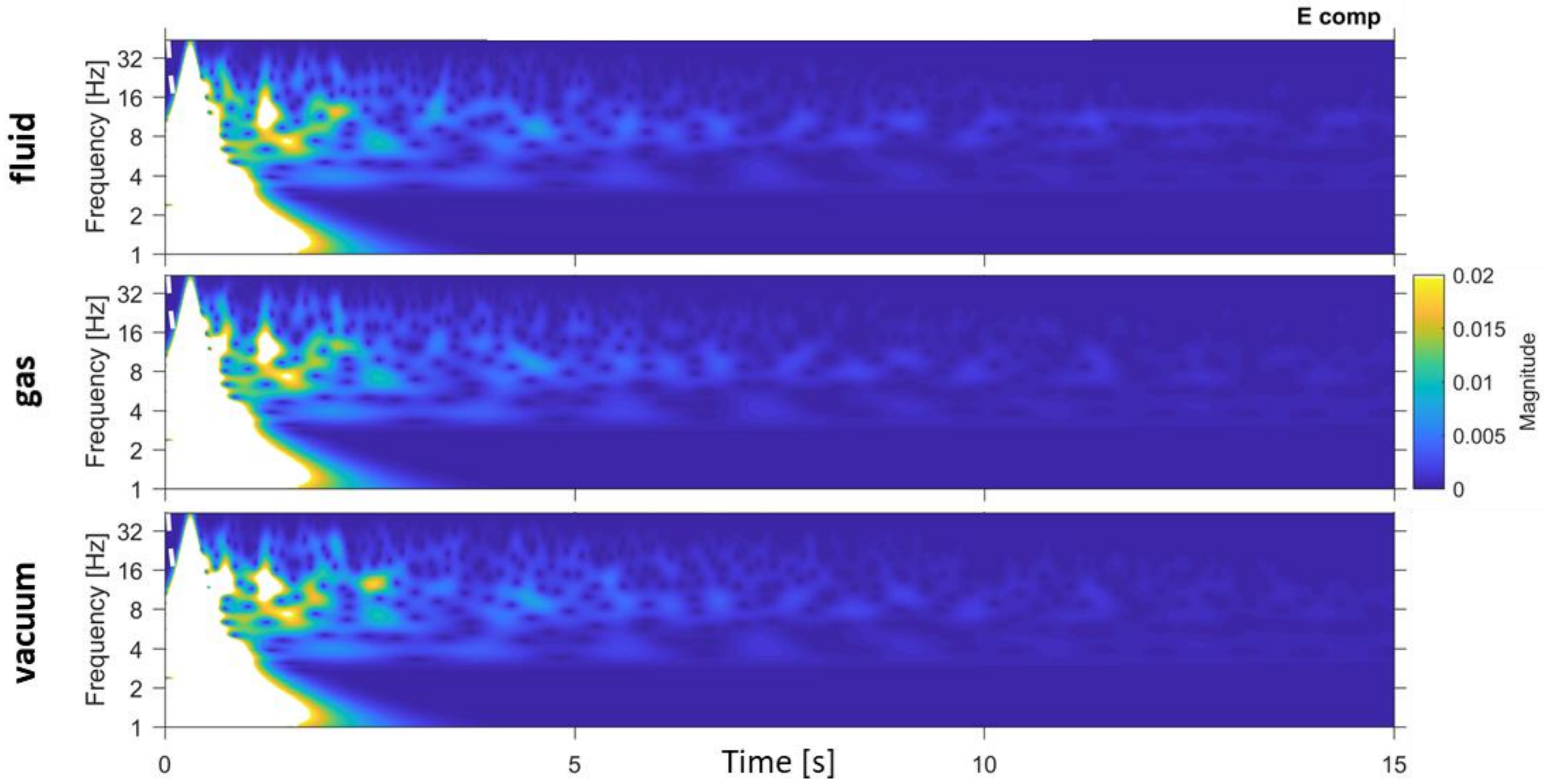

The effects of cavity/apical-void filling

Select

Mediu

- tuff (model
- rock salt

Comp

- horizontal E
- vertical

Receiver posit
[center of cavit

Type of e
plane S-w

Low yie

Minimal depth o

elastic mode

Differences are visible but not significant.

The overall character of TFRs is basically the same.
TFRs mainly differ in frequencies that are enhanced.

The differences due to the type of filling
are better visible in the models without chimney.

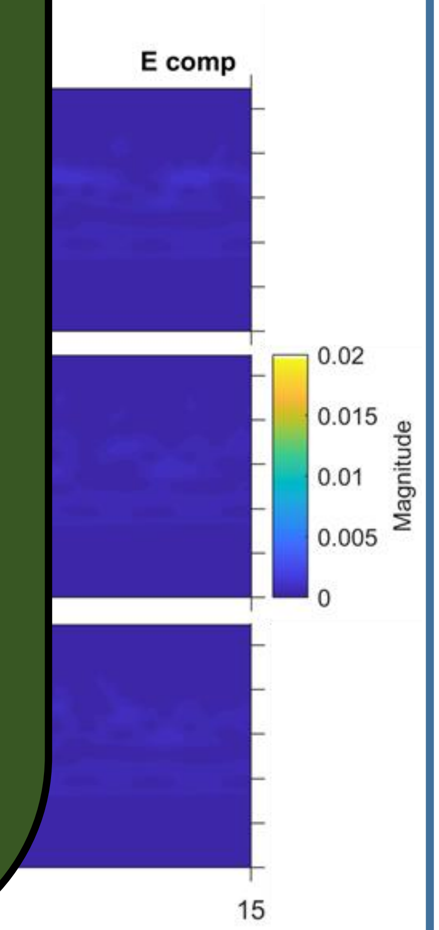

Results of analysis

- the effects of cavity/apical-void filling
- **the effects of attenuation**
- analysis of seismic wavefields due to regional and distant seismic sources
- analysis of seismic wavefields due to weak local aftershocks
- analysis of simulated ambient noise

The effects of attenuation

Comparison of the effect of **attenuation** on time-frequency representations of seismograms

Select

Cavity / Apical void

- ○ fluid-filled
- ○ gas-filed
- ◉ vacuum

Receiver position (-200,0) m
[center of cavity is at (0, 0) m]

Type of excitation
plane S-wave (EW)

Low yield (1kt)

Minimal depth of burial (180m)

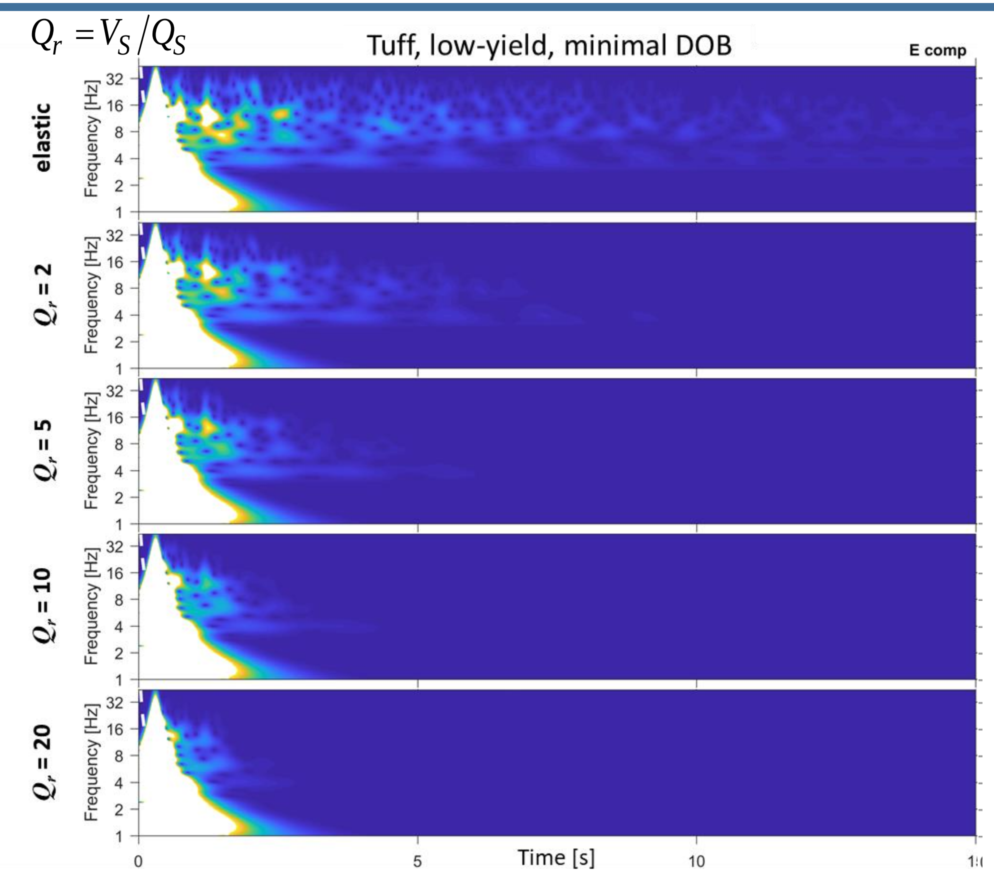

The effects of attenuation

Comparison of the effect of **attenuation** on time-frequency representations of seismograms

Select

Cavity / Apical void

- ○ fluid-filled
- ○ gas-filed
- ◉ vacuum

Receiver position (-200,0) m
[center of cavity is at (0, 0) m]

Type of excitation
plane S-wave (EW)

Low yield (1kt)

Minimal depth of burial (180m)

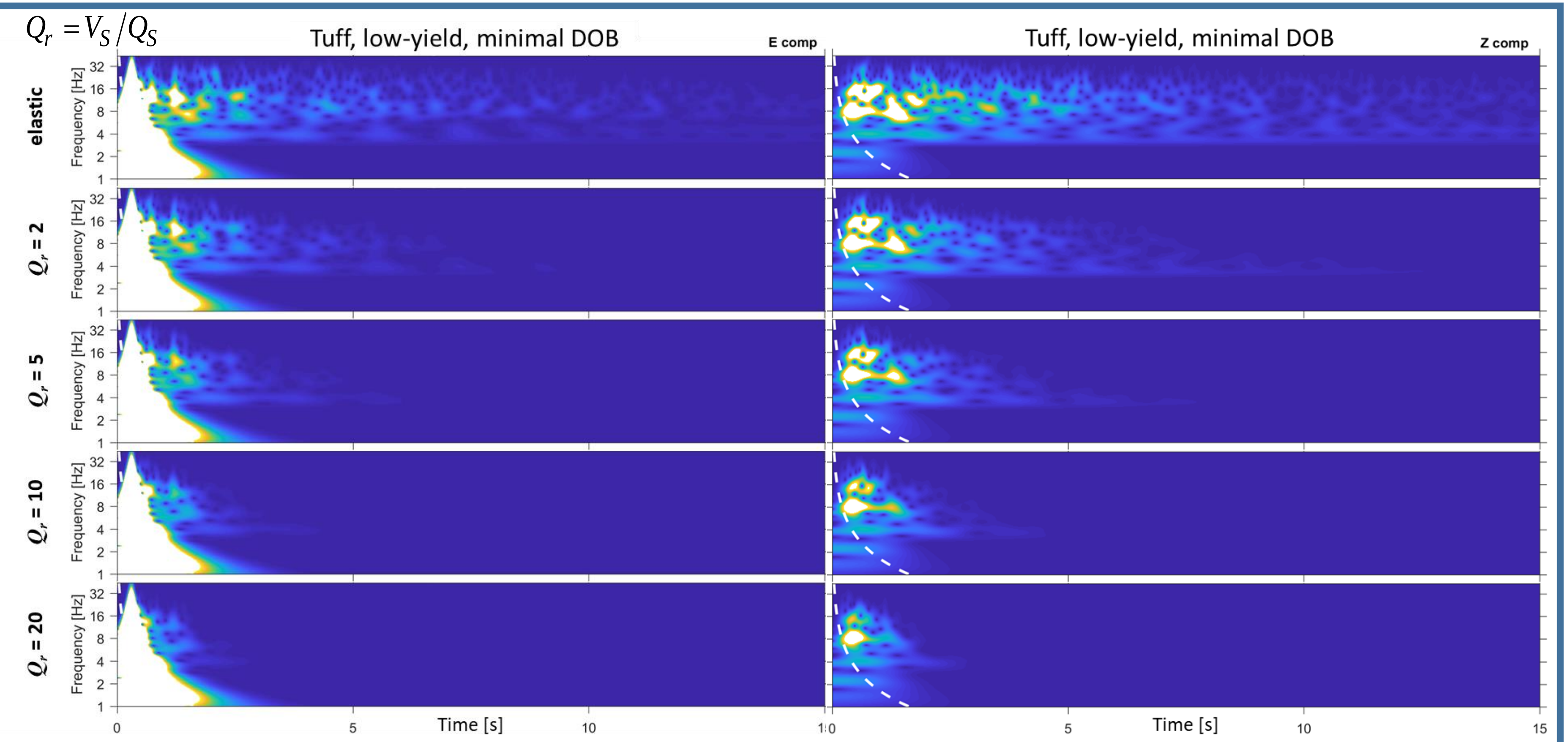

The effects of attenuation

Comparison of the effect of **attenuation** on time-frequency representations of seismograms

Select

Cavity / Apical void

- ○ fluid-filled
- ○ gas-filed
- ● vacuum

Receiver position (-200,0) m

[center of cavity is at (0, 0) m]

Type of excitation

plane S-wave (EW)

Low yield (1kt)

Minimal depth of burial (180m)

$Q_r = V_S / Q_S$

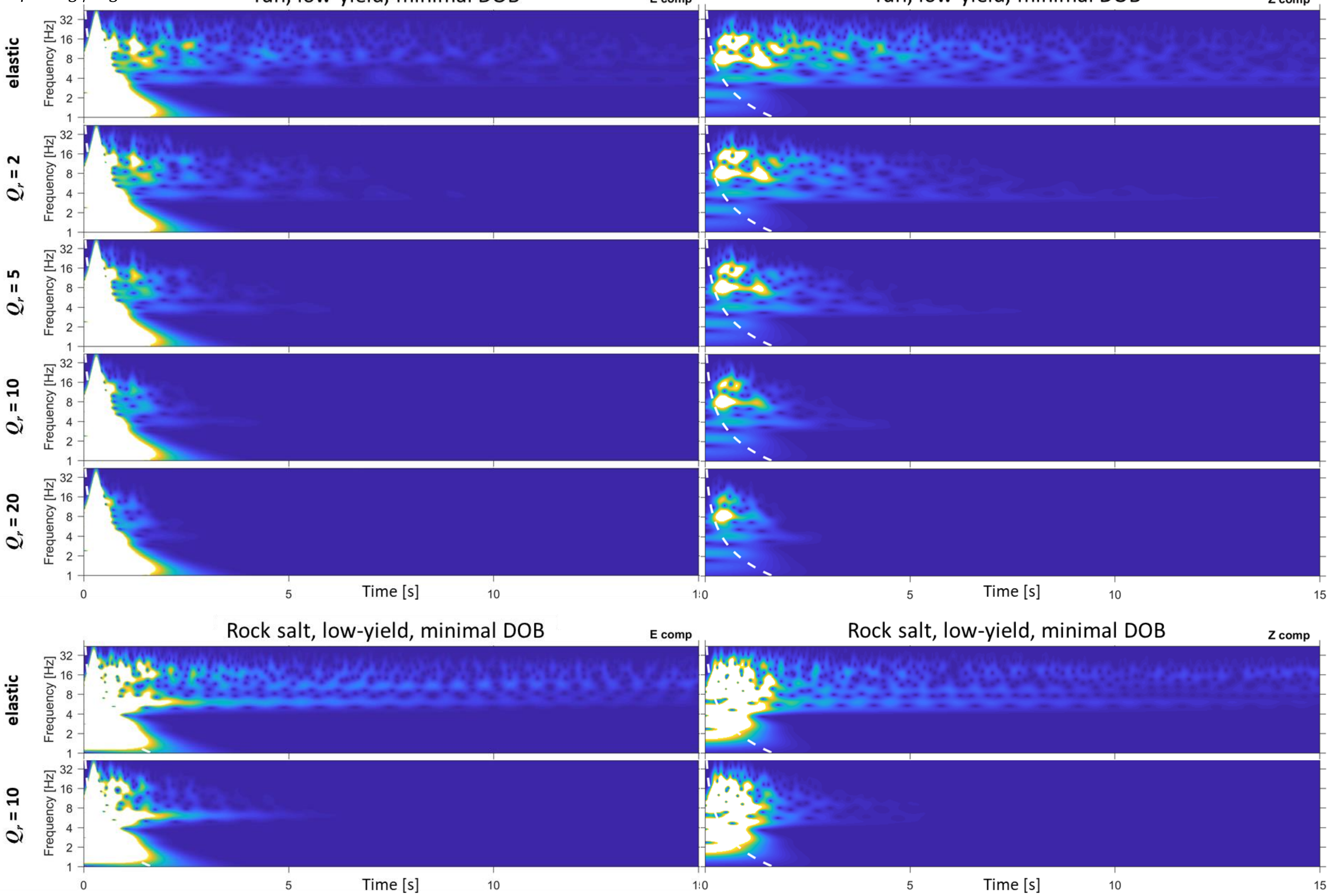

The effects of attenuation

$Q_r = V_S / Q_S$

Comparison of t
of atten
time-frequen
of se

Cavity
fluid-fil
gas-file
vacuum

Receiver p
[center o

Type
plane

Low

Minimal depth o

The attenuation mainly affects the coda of seismograms.

Higher frequencies are more attenuated.

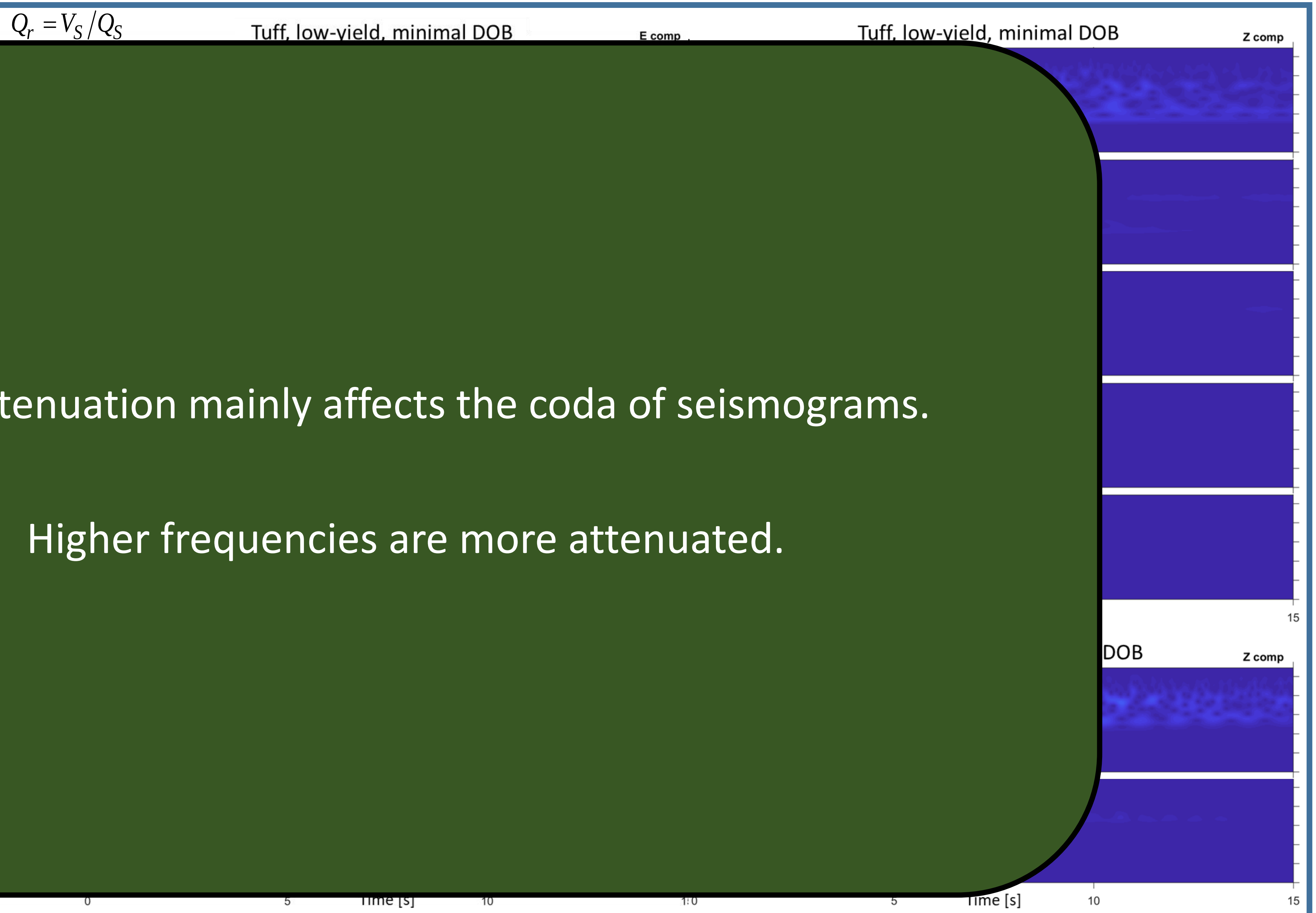

Results of analysis

- the effects of cavity/apical-void filling
- the effects of attenuation
- **analysis of seismic wavefields due to regional and distant seismic sources**
- analysis of seismic wavefields due to weak local aftershocks
- analysis of simulated ambient noise

analysis of simulated realistic seismograms

we convolved the synthetic Fourier transfers functions
with real (recorded) accelerograms (differing in spectral content)

RESORCE waveform ID and station name	Label	Earthquake (Name, date, magnitude)	Epicentral Distance (km)	Component	Pga (cm/s²)	Fpeak (Hz)	Source
14683 Borgo Cerreto – Torre	**RA1**	Umbria-Marche 14/10/1997 15:23, **Mw 5.6**	**9**	H1	333	4.6	ITACA
				H2	329	3.3	
				V	157		
6756 - Flagbjarnarholt	**RA2**	South-Iceland, 17/06/2000 15:40, **Mw 6.5**	**20**	H1	315	2.5	ESMD
				H2	339	10.0	
				V	271		
15905 - Zarrat	**RA3**	Firuzabad, 20/06/1994 09:09, **Mw 5.9**	**16**	H1	301	4.2	ESMD
				H2	253	4.6	
				V	102		
16996 - L'Aquila - V. Aterno - Il Moro - AQM	**RA4**	L'Aquila Aftershock 07/04/2009 21:34, **Mw 4.6**	**2**	H1	247	8.3	ITACA
				H2	130	50	
				V	82		
17116 – Montereale - MTR	**RA5**	L'Aquila Aftershock 09/04/2009 19:38, **Mw 5.3**	**10**	H1	108	10	ITACA
				H2	90	20	
				V	67		

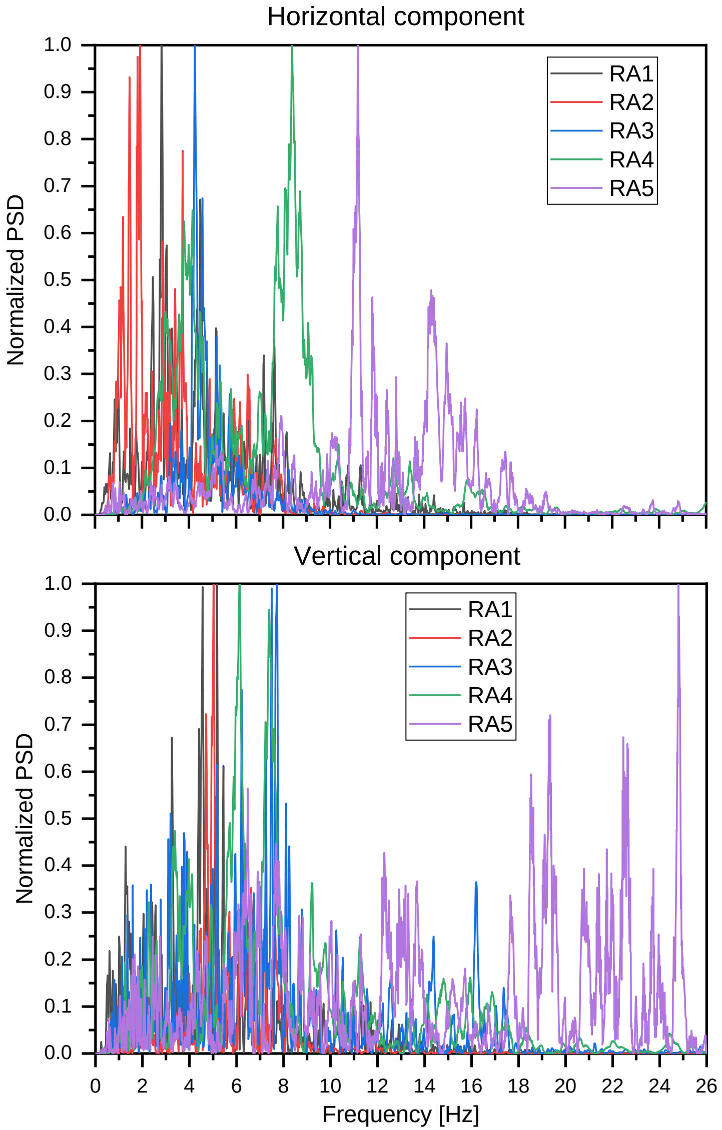

analysis of simulated realistic seismograms

Median frequency (SEF 50%) (low-yield, fluid-filled cavity/apical void)

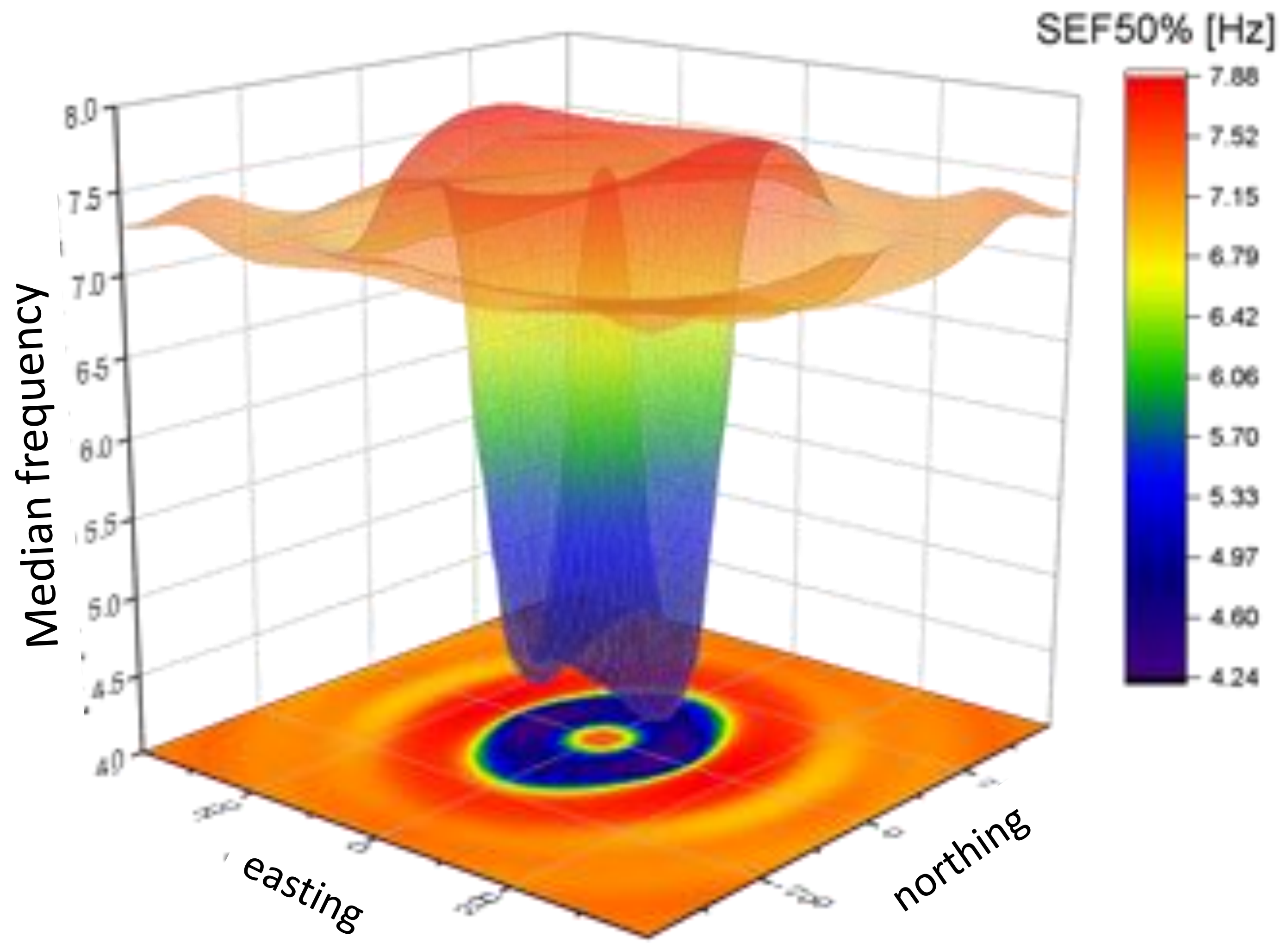

Select:

Medium

◉ tuff (model with chimney) ○ rock salt

Depth of burial

◉ minimal (180m) ○ 2 x minimal (360m)

analysis of simulated realistic seismograms

Median frequency (SEF 50%) (low-yield, fluid-filled cavity/apical void)

	RA1	RA2	RA3	RA4	RA5
Horizontal	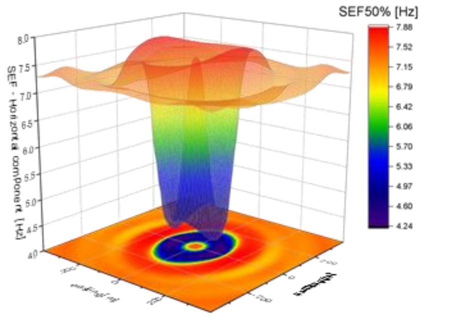	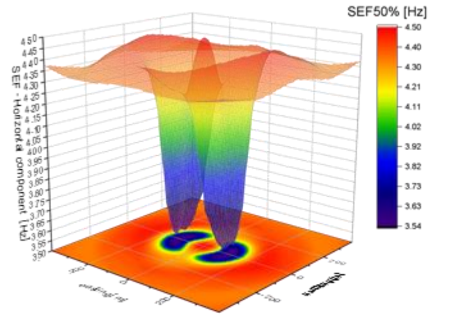	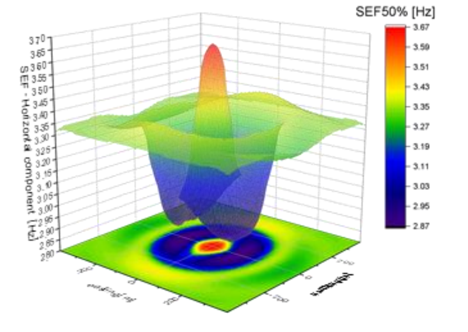	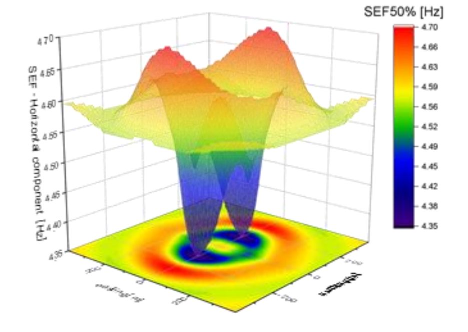	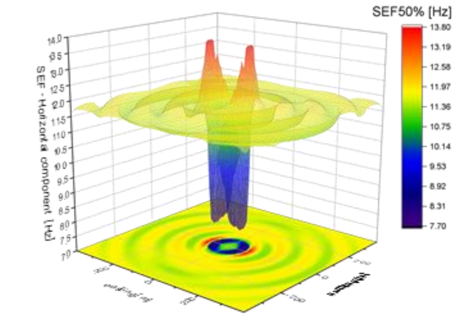

Select:

Medium

◉ tuff (model with chimney) ○ rock salt

Depth of burial

◉ minimal (180m) ○ 2 x minimal (360m)

analysis of simulated realistic seismograms

Median frequency (SEF 50%) (low-yield, fluid-filled cavity/apical void)

	RA1	RA2	RA3	RA4	RA5
Horizontal	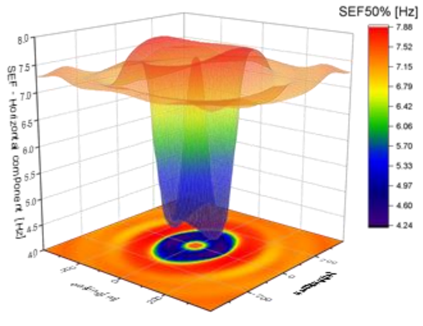	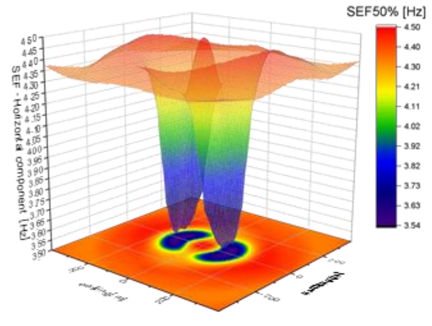	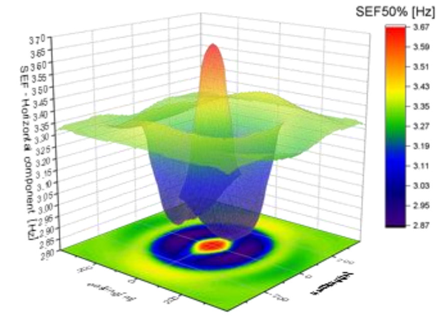	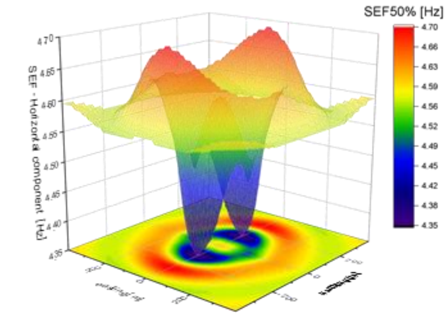	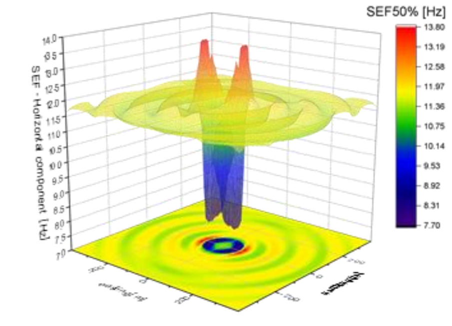
Vertical	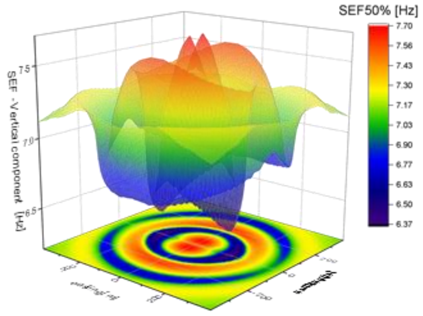	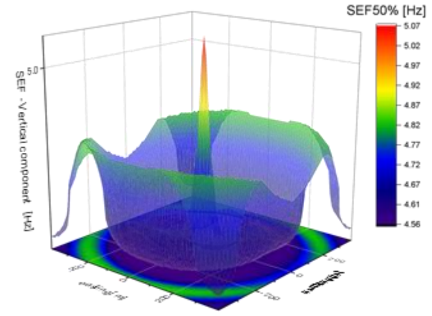	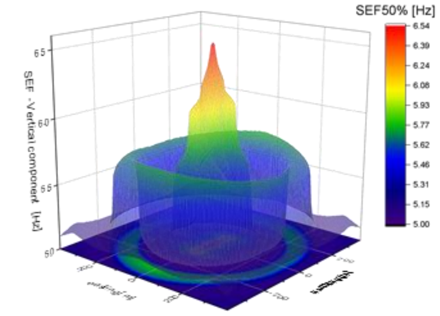	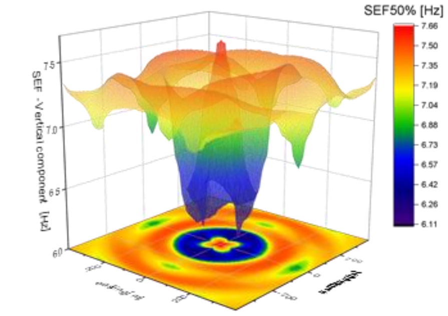	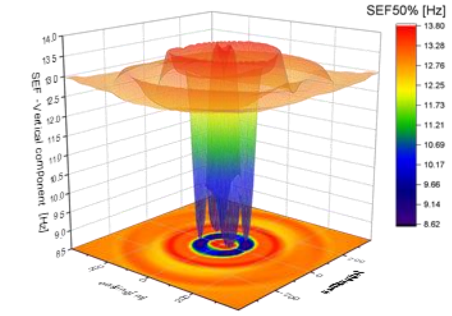

Select:

Medium

◉ tuff (model with chimney) ○ rock salt

Depth of burial

◉ minimal (180m) ○ 2 x minimal (360m)

analysis of simulated realistic seismograms

Median frequency (SEF 50%) (low-yield, fluid-filled cavity/apical void)

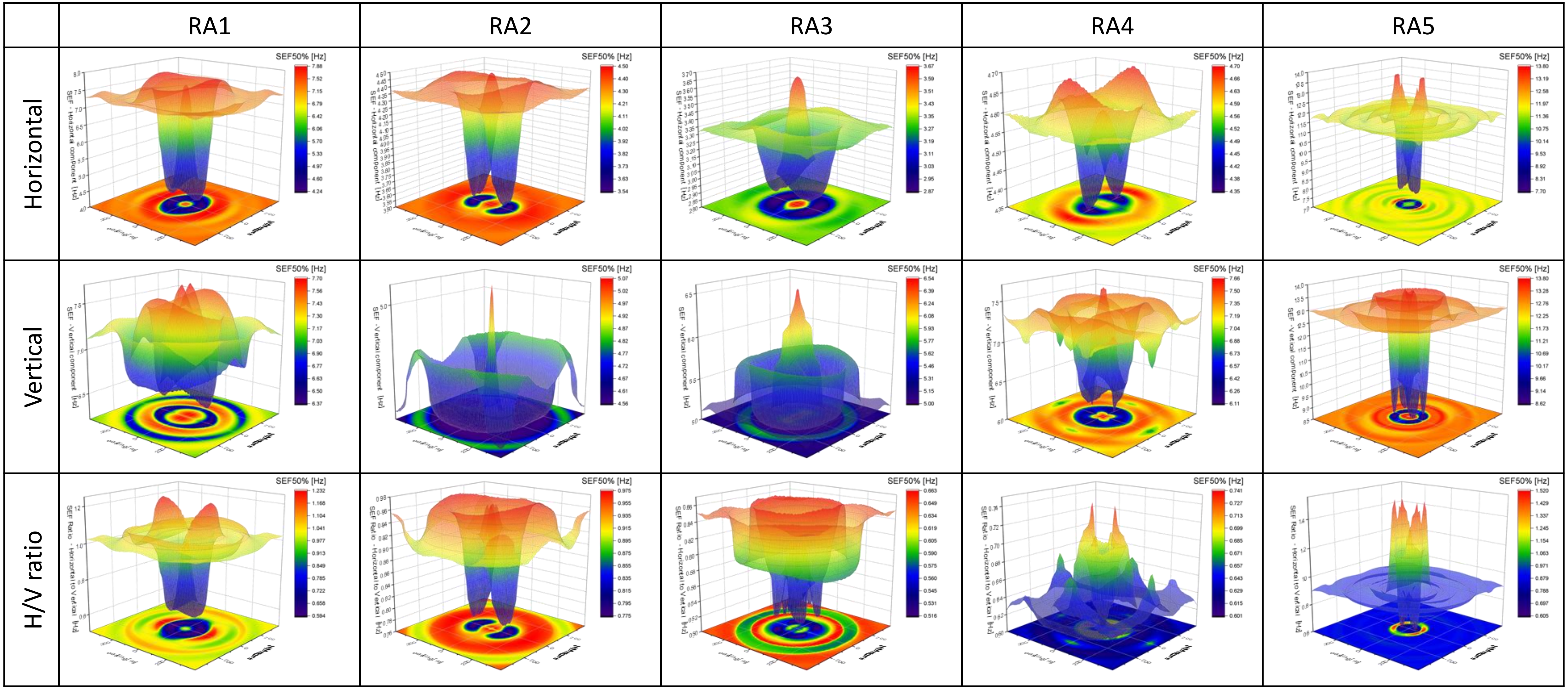

Select:

Medium

◉ tuff (model with chimney) ○ rock salt

Depth of burial

◉ minimal (180m) ○ 2 x minimal (360m)

analysis of simulated realistic seismograms

Median frequency (SEF 50%) (low-yield, fluid-filled cavity/apical void)

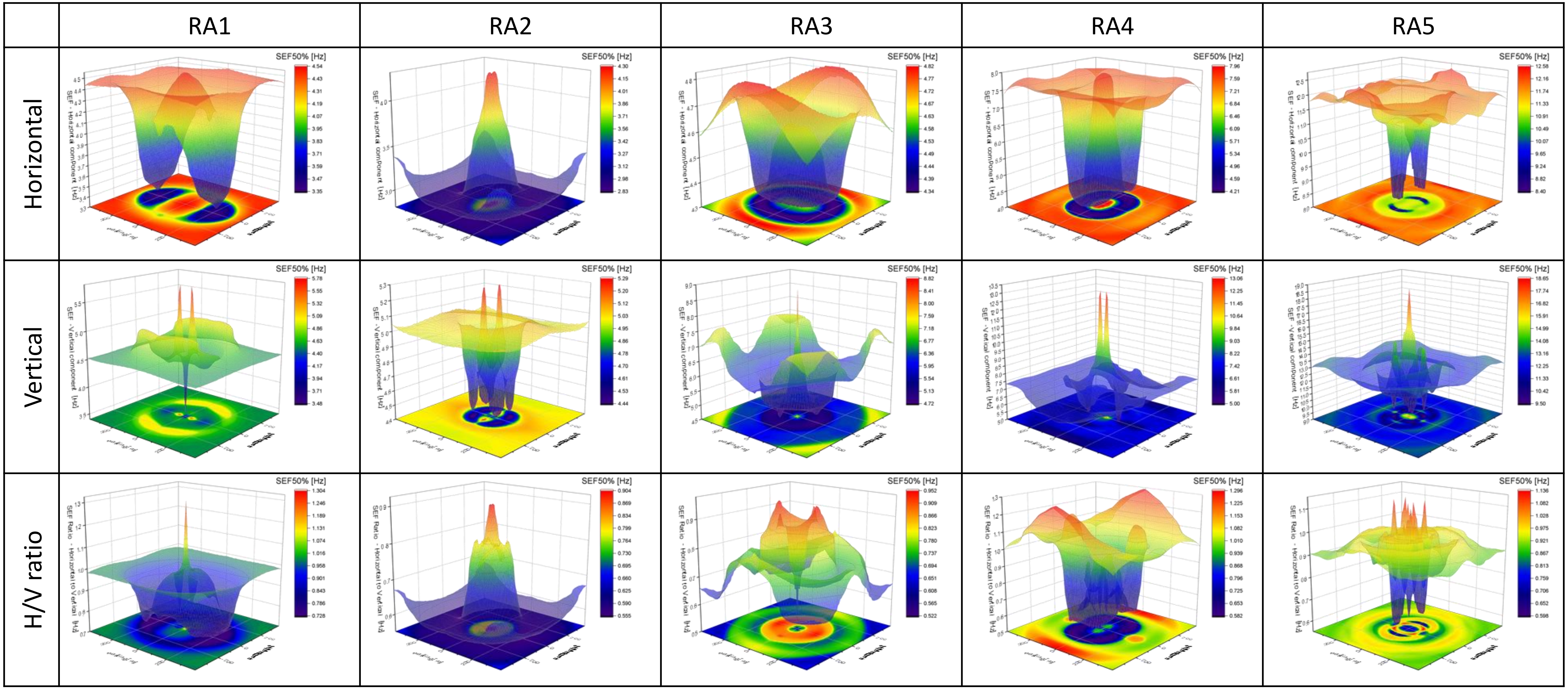

Select:

Medium

○ tuff (model with chimney) ◉ rock salt

Depth of burial

◉ minimal (180m) ○ 2 x minimal (360m)

analysis of simulated realistic seismograms

Median frequency (SEF 50%) (low-yield, fluid-filled cavity/apical void)

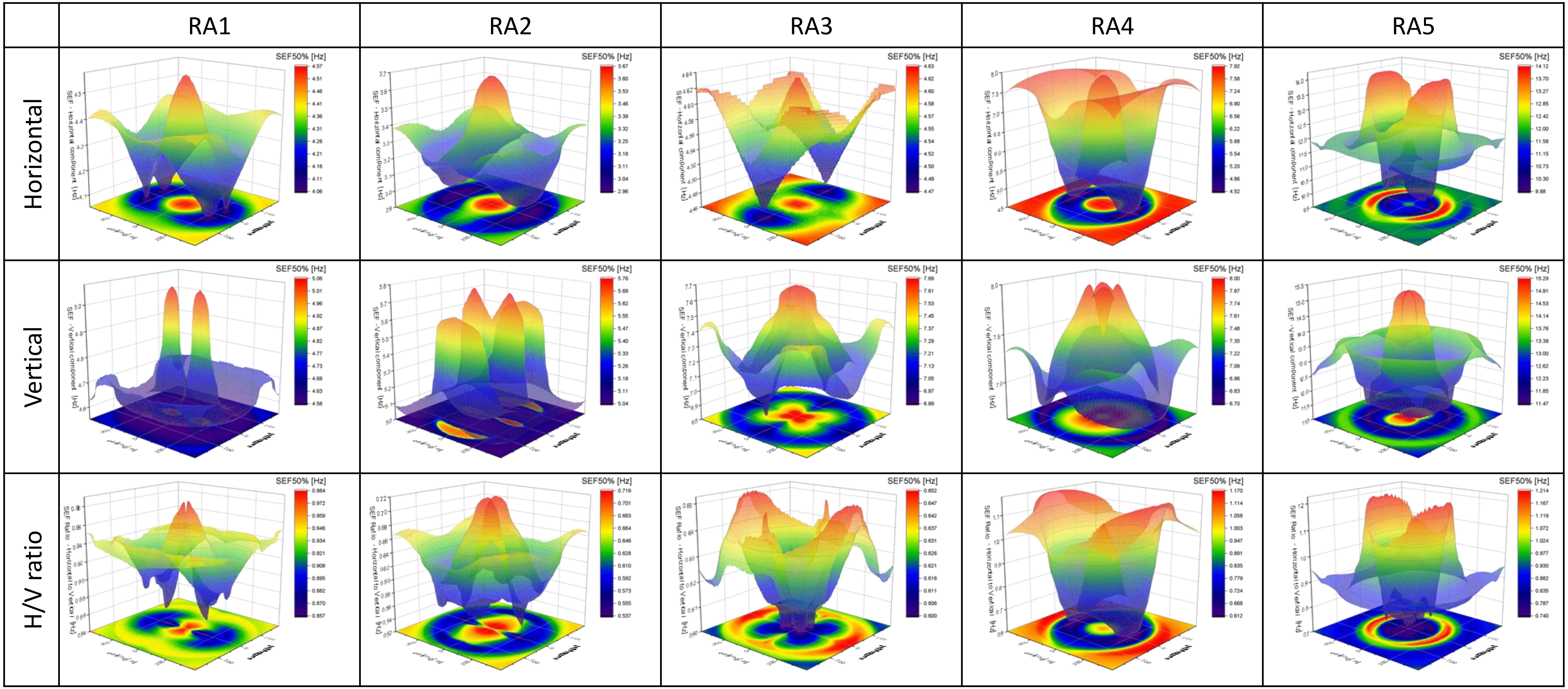

Select:

Medium

○ tuff (model with chimney) ◉ rock salt

Depth of burial

○ minimal (180m) ◉ 2 x minimal (360m)

analysis of simulated realistic seismograms

Median frequency (SEF 50%) (low-yield, fluid-filled cavity/apical void)

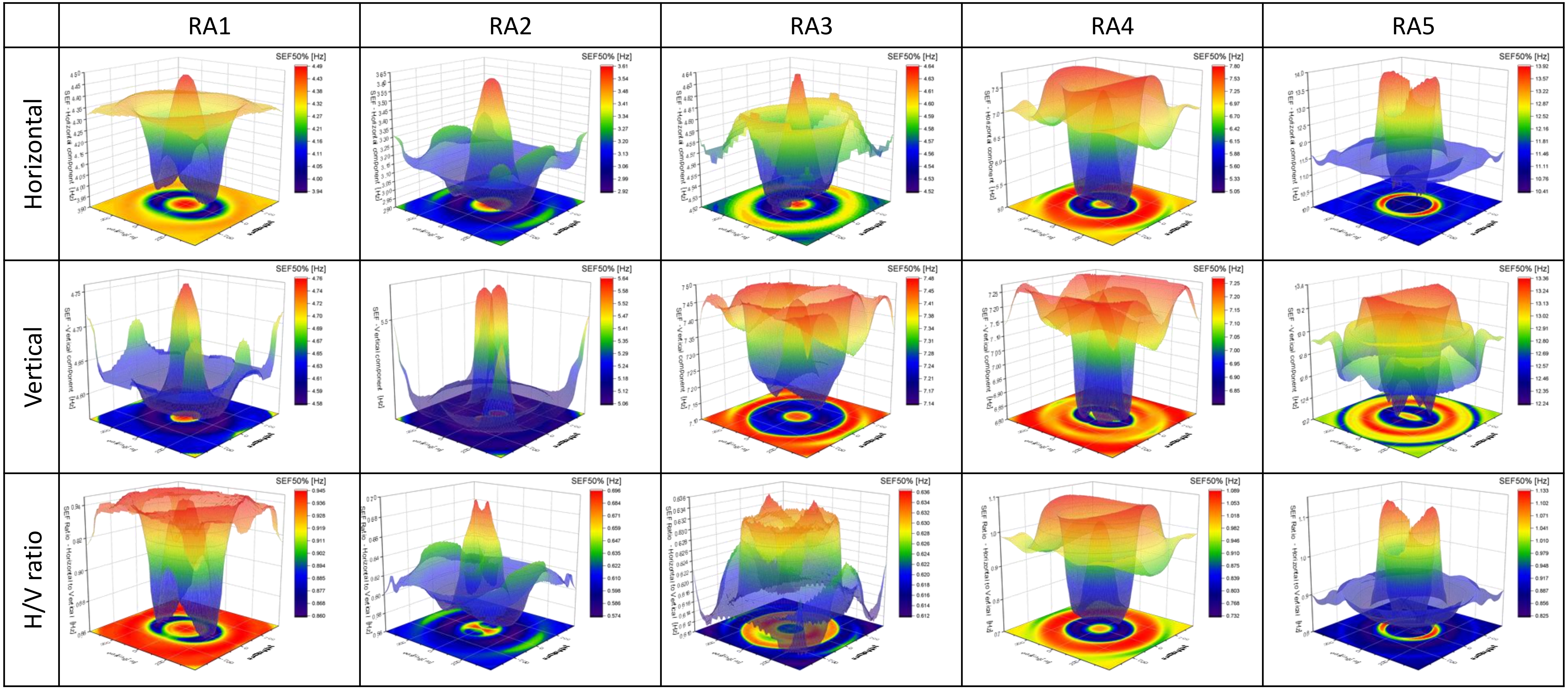

Select:

Medium

◉ tuff (model with chimney) ○ rock salt

Depth of burial

○ minimal (180m) ◉ 2 x minimal (360m)

analysis of simulated realistic seismograms

Median frequency (SEF 50%) (low-yield, fluid-filled cavity/apical void)

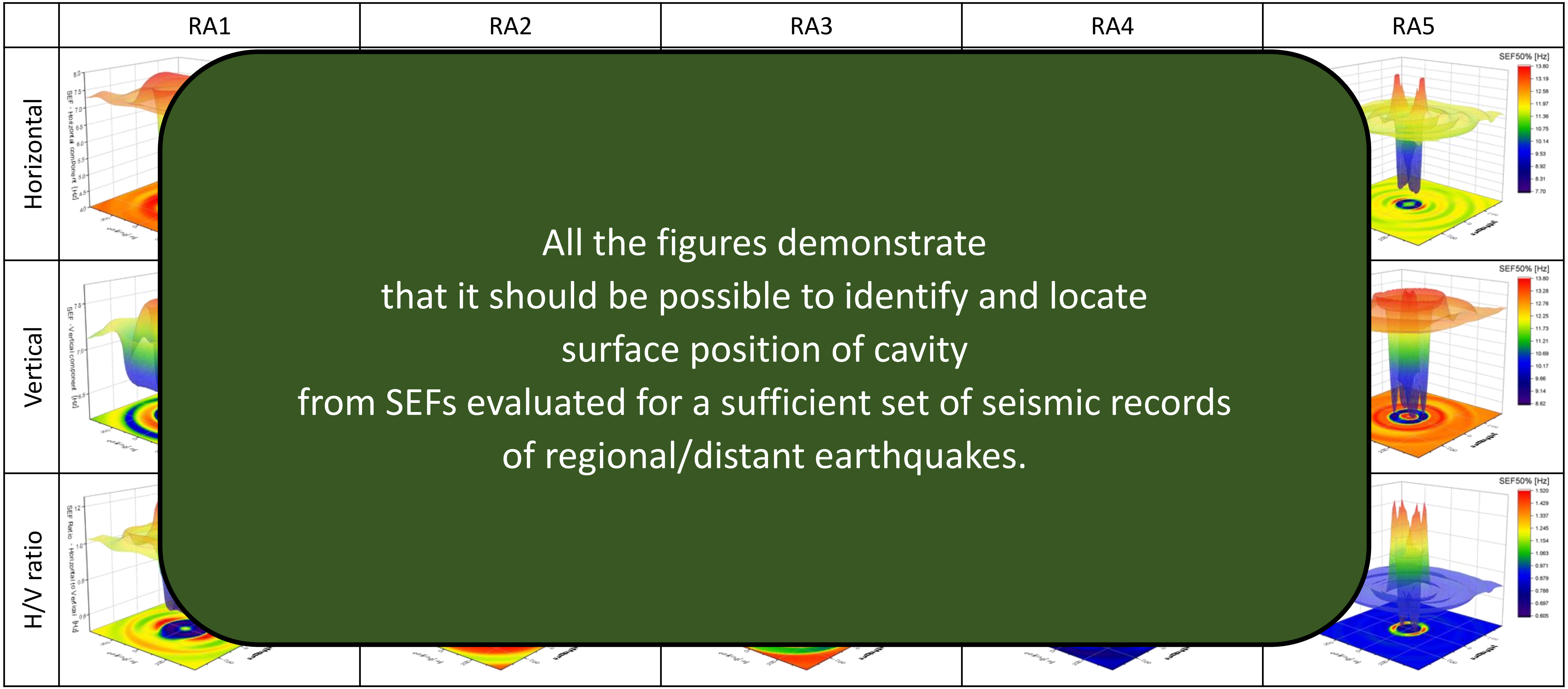

All the figures demonstrate
that it should be possible to identify and locate
surface position of cavity
from SEFs evaluated for a sufficient set of seismic records
of regional/distant earthquakes.

Select:

Medium

◉ tuff (model with chimney) ○ rock salt

Depth of burial

◉ minimal (180m) ○ 2 x minimal (360m)

Results of analysis

- the effects of cavity/apical-void filling

- the effects of attenuation

- analysis of seismic wavefields due to regional and distant seismic sources

- **analysis of seismic wavefields due to weak local aftershocks**

- analysis of simulated ambient noise

analysis of wavefields due to point double-couple sources (aftershocks)

tuff, low-yield, fluid-filled apical void, minimal DOB

Median frequency (SEF 50%)

aerial view

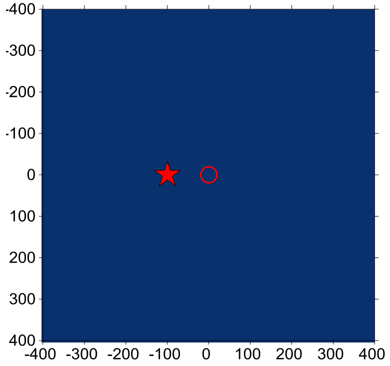

cross section

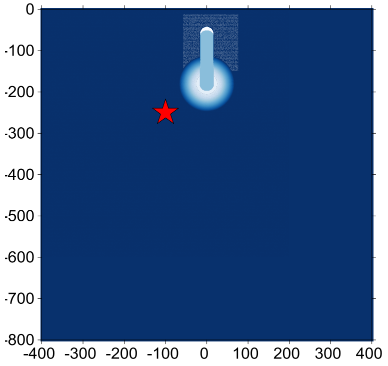

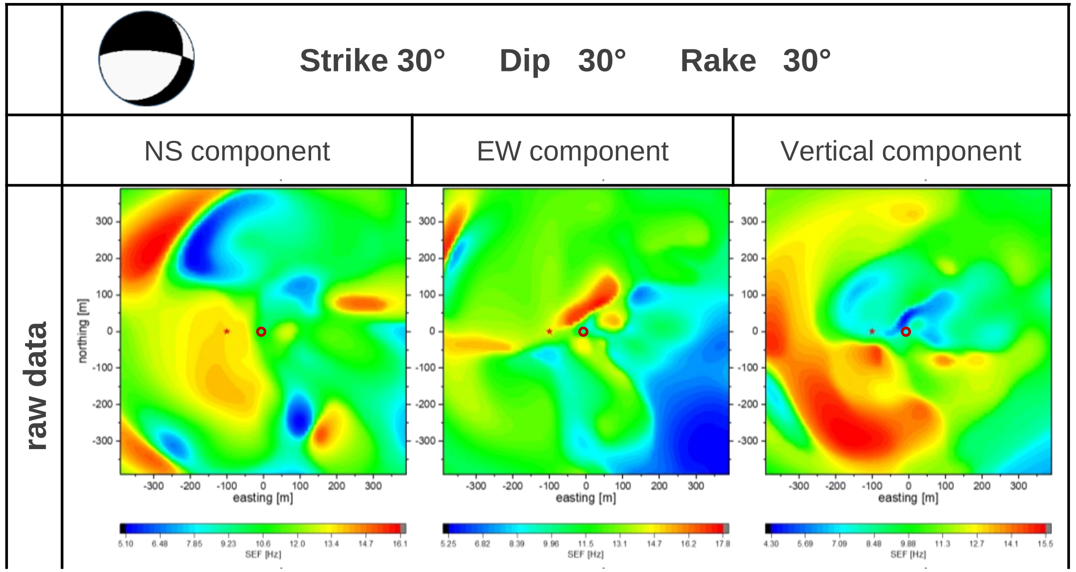

analysis of wavefields due to point double-couple sources (aftershocks)

tuff, low-yield, fluid-filled apical void, minimal DOB

aerial view

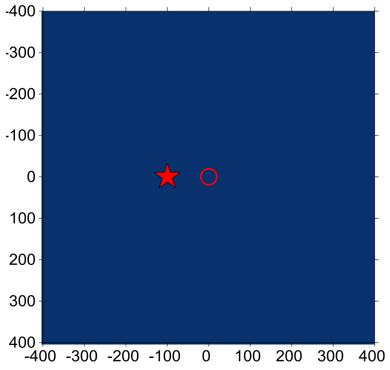

cross section

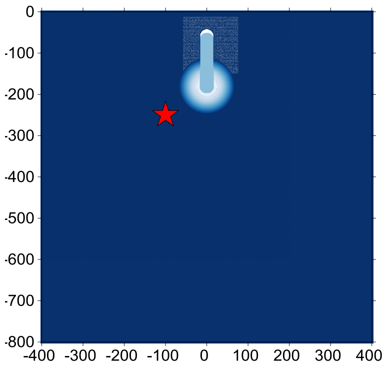

Median frequency (SEF 50%)

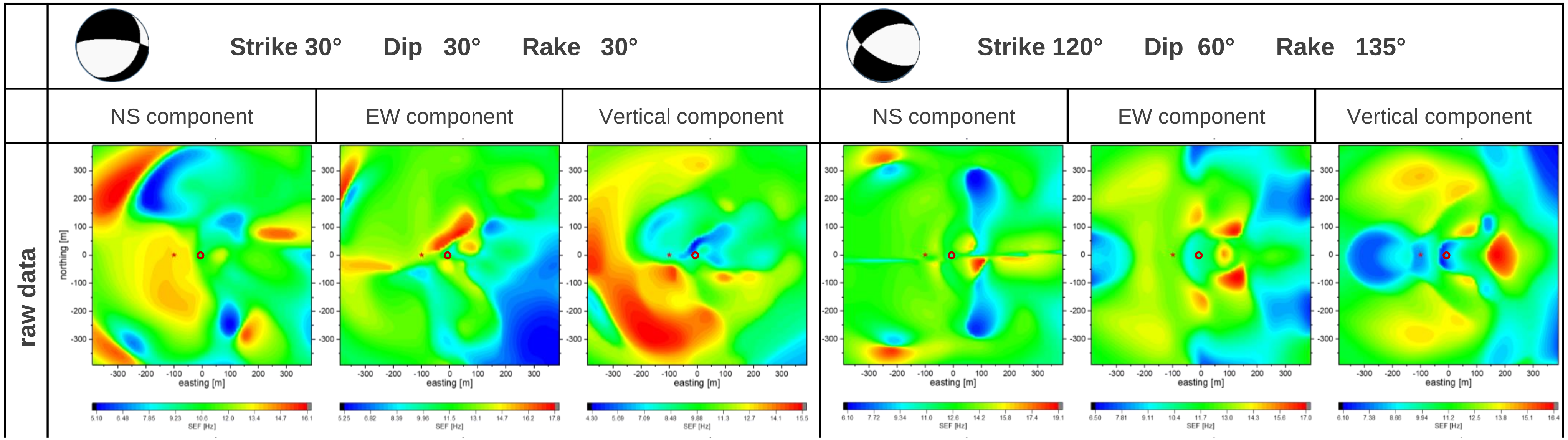

analysis of wavefields due to point double-couple sources (aftershocks)

tuff, low-yield, fluid-filled apical void, minimal DOB

Median frequency (SEF 50%)

aerial view

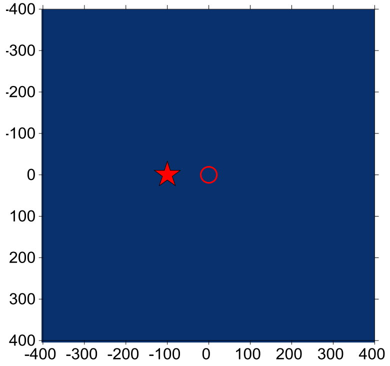

cross section

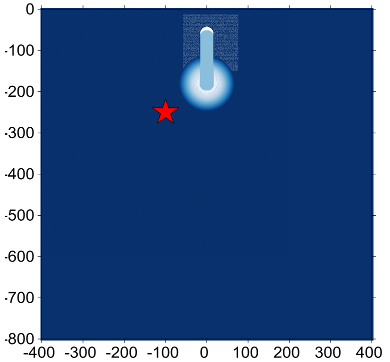

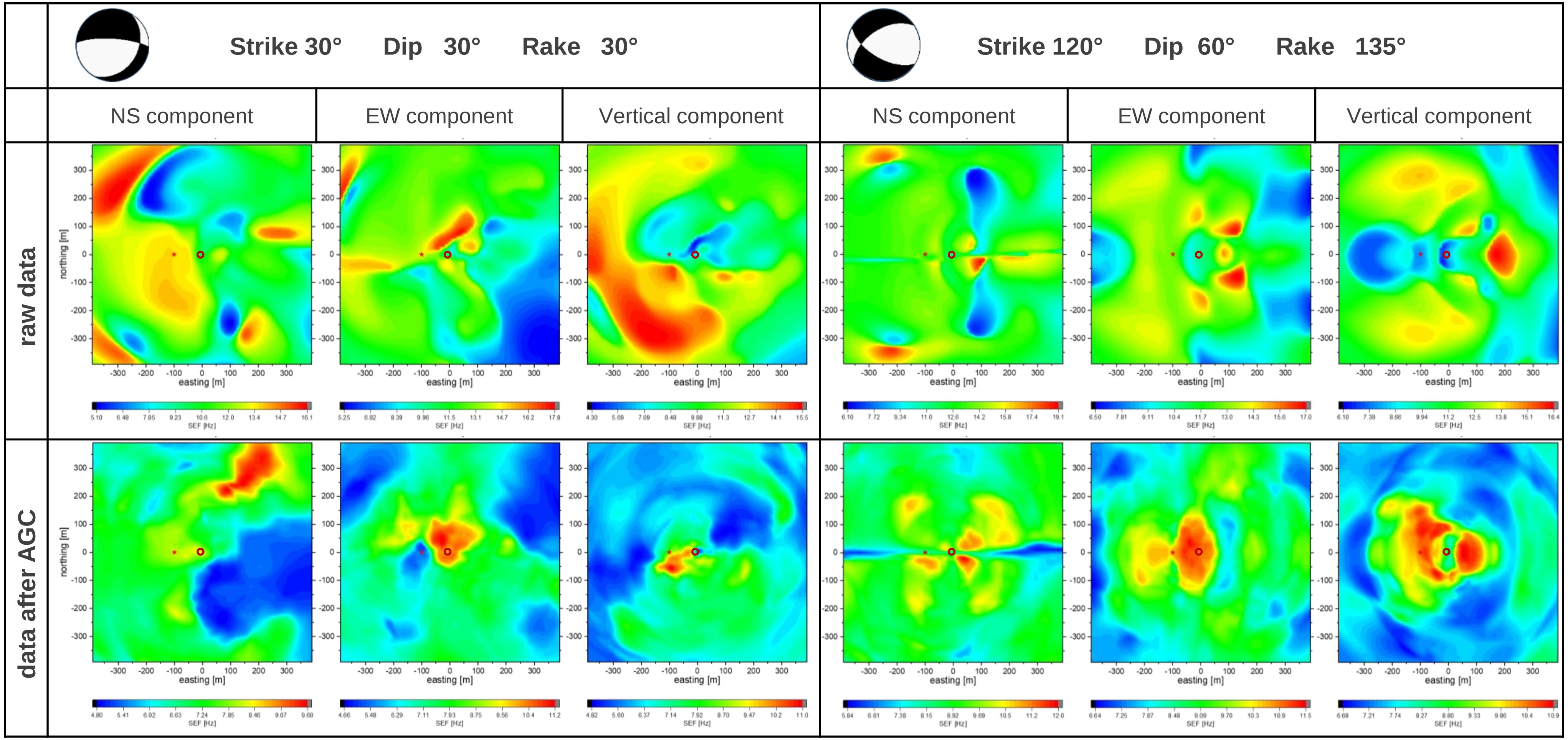

analysis of wavefields due to point double-couple sources (aftershocks)

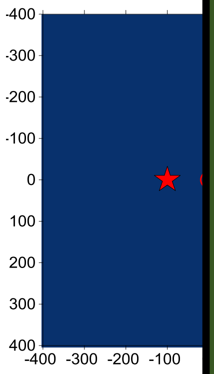

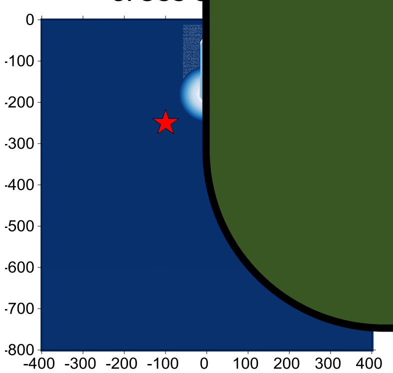

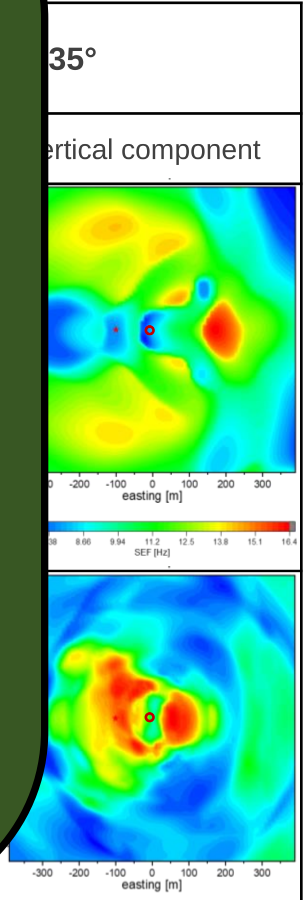

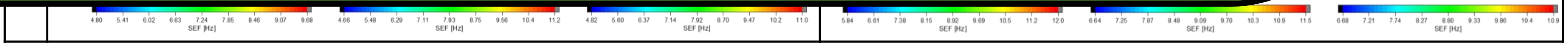

A seismic wavefield due to a near aftershock
is too much affected or dominated by the radiation patterns
of the source.

This makes identification of cavity signatures very difficult
from records of a single aftershock.

Results of analysis

- the effects of cavity/apical-void filling
- the effects of attenuation
- analysis of seismic wavefields due to regional and distant seismic sources
- analysis of seismic wavefields due to weak local aftershocks
- **analysis of simulated ambient noise**

Analysis of simulated ambient noise

Due to large computational requirements,
one numerical simulation of seismic noise provided maximum 4.5 min of noise.
Still not enough, because in practice
several tens of minutes (and even longer) of seismic records are used.

Therefore we tried to estimate
whether there is any hidden information about cavity position in spectrum
that could be extracted if sufficiently long noise records were available.

Analysis of simulated ambient noise

Due to large computational requirements,
one numerical simulation of seismic noise provided maximum 4.5 min of noise.
Still not enough, because in practice
several tens of minutes (and even longer) of seismic records are used.

Therefore we tried to estimate
whether there is any hidden information about cavity position in spectrum
that could be extracted if sufficiently long noise records were available.

We calculated
a relative Power –
Power evaluated from the difference
between
the complex Fourier spectra evaluated
for the seismic noise in the UNE-altered medium
and
for the seismic noise in the original (before UNE)
homogeneous halfspace.

Analysis of simulated ambient noise

Relative Power

Select

Model
low yield

◉ tuff (with chimney)

○ rock salt

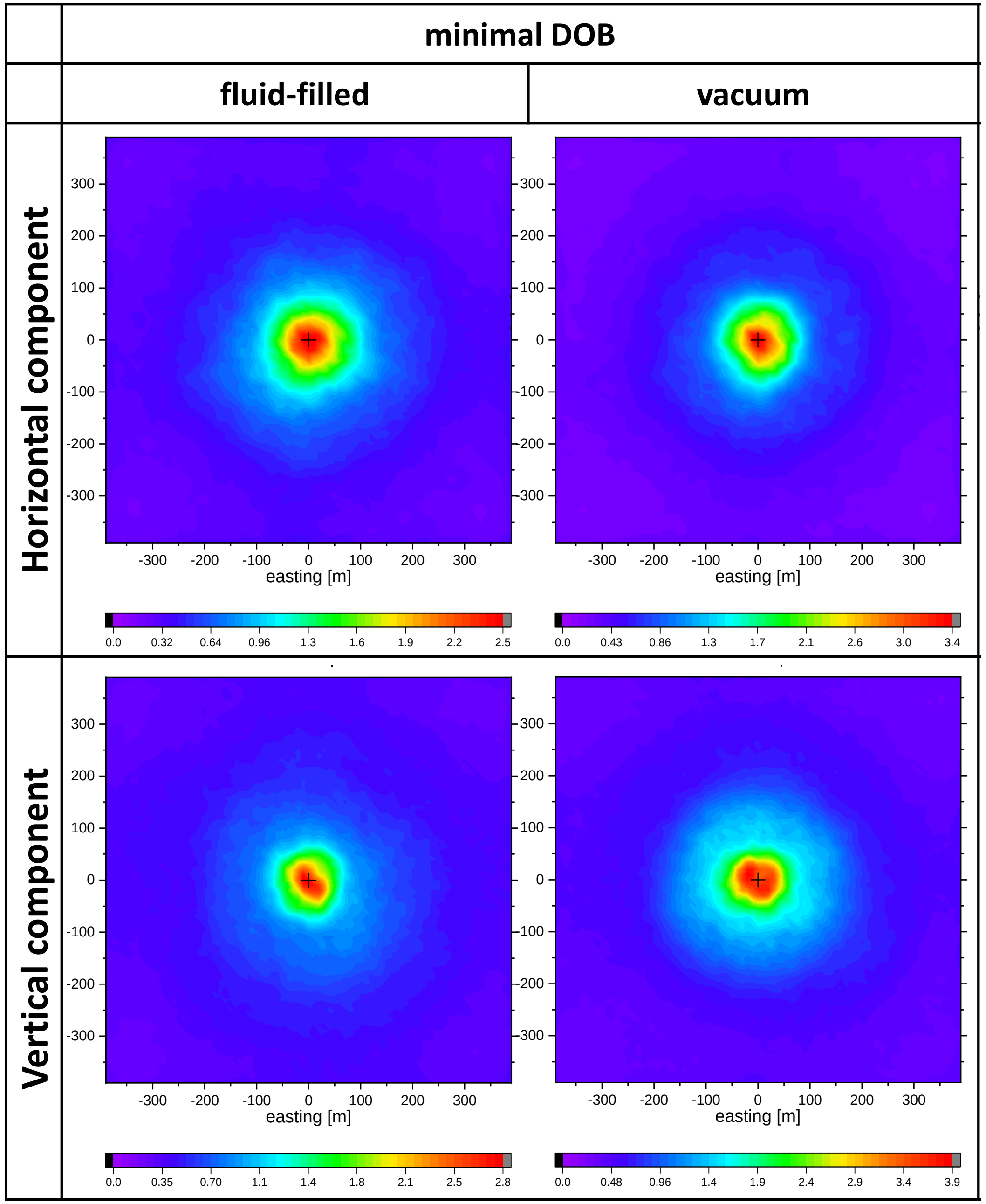

Analysis of simulated ambient noise

Relative Power

Select

Model

low yield

◉ tuff (with chimney)

○ rock salt

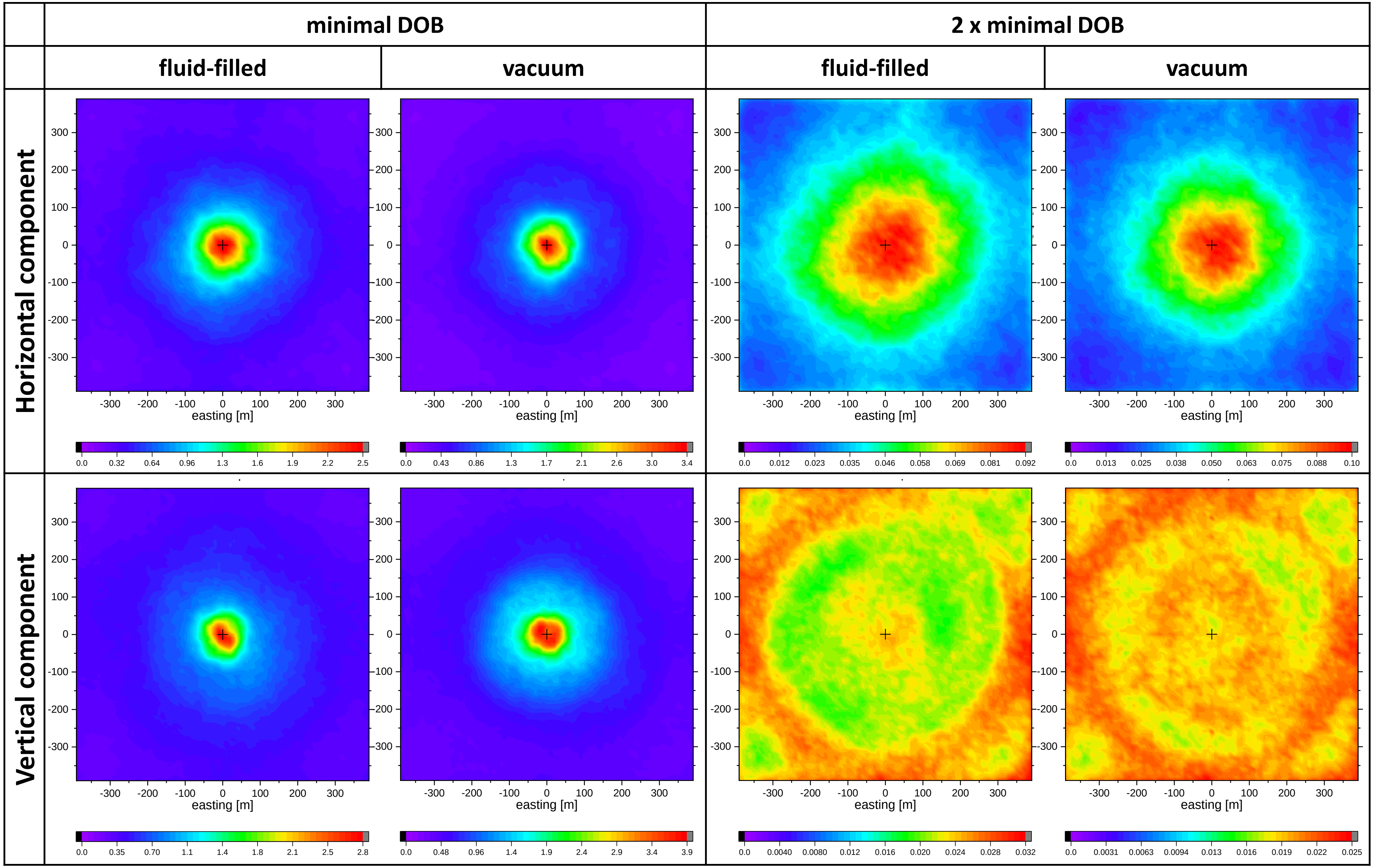

Analysis of simulated ambient noise

Relative Power

Select

Model

low yield

○ tuff (with chimney)

◉ rock salt

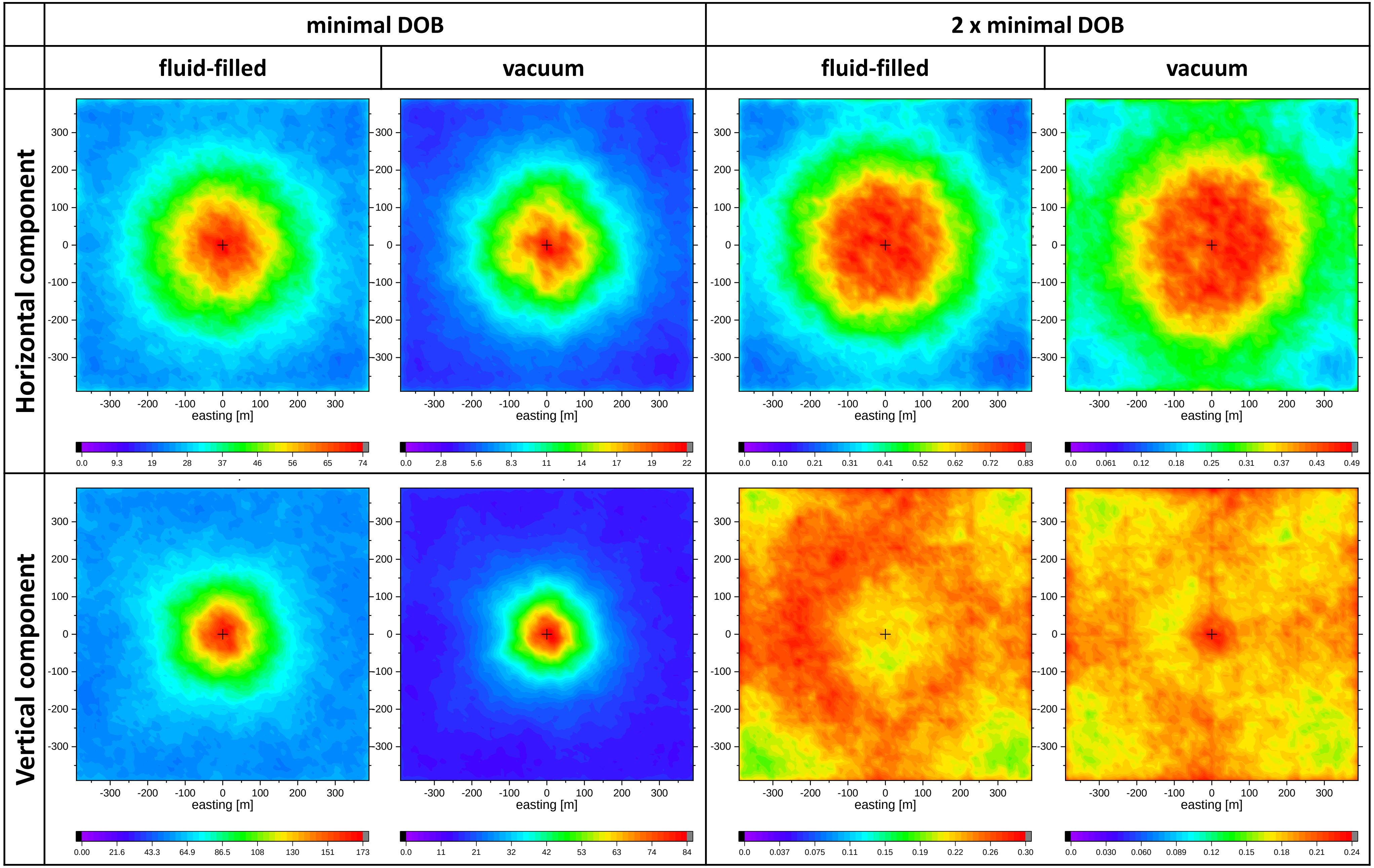

Analysis of simulated ambient noise

Relative Power

Select

Scaling

- (●) local, linear
- ( ) global, logarithmic

Model
low yield

- (●) tuff (with chimney)
- ( ) rock salt

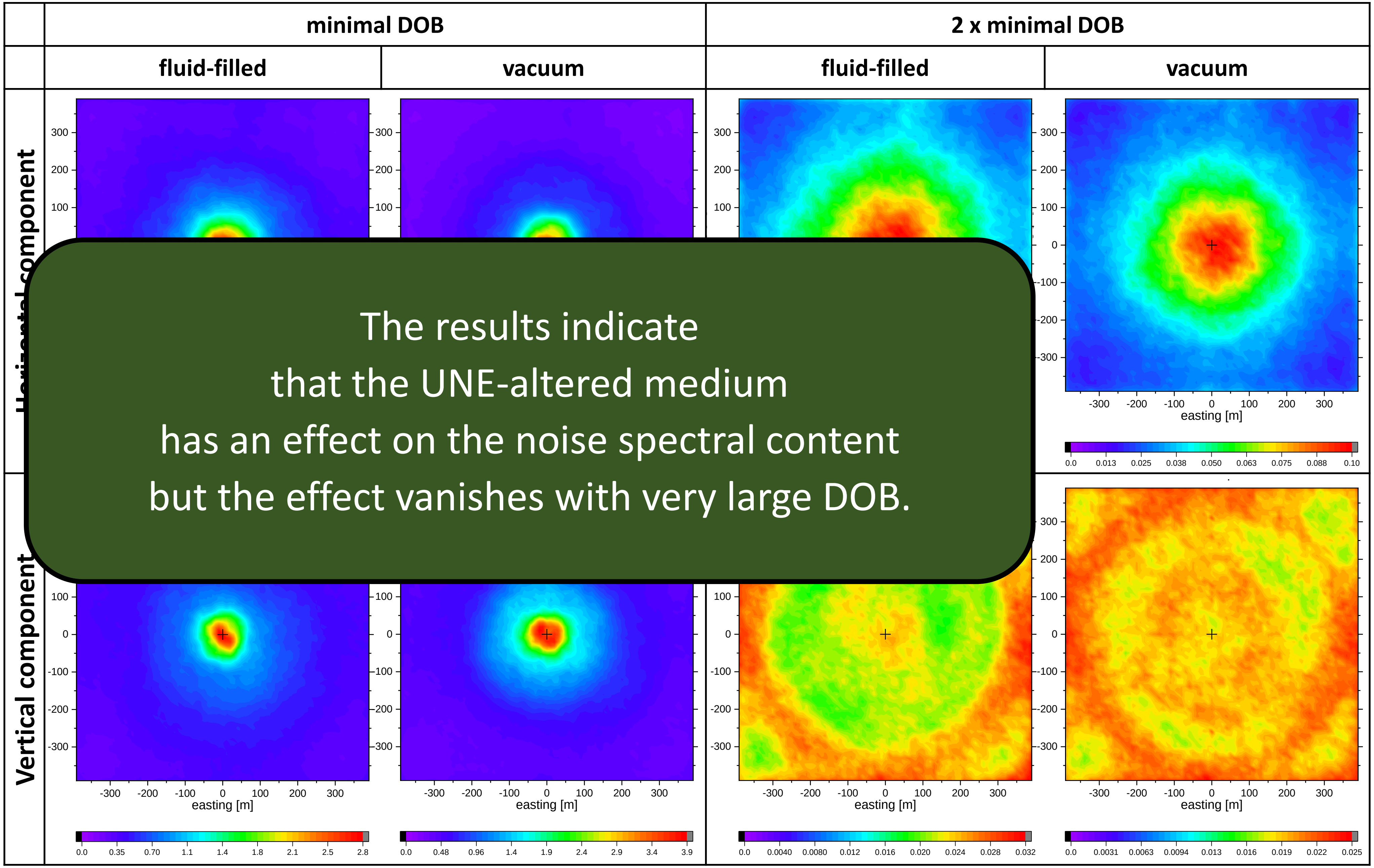

The results indicate
that the UNE-altered medium
has an effect on the noise spectral content
but the effect vanishes with very large DOB.

Conclusions (1/3)

- **We have developed a set of realistic structural models**
  of the underground structure
  after an underground nuclear explosion.

- **We performed an extensive numerical simulations**
  of seismic wavefields due to
  plane-wave excitation,
  point double-couple sources,
  and random ambient noise sources
  using forward 3D finite-difference method.

Conclusions (2/3)

- **TFRs and FTFs**, though having similar patterns for different models (type of the rock environment, filling of the cavity/apical void), **indicate various specific frequencies at which seismic motion is excited/amplified** due to different model parameters.

- We showed that the **characteristics of SEFs provide a robust tool** for identifying redistribution of energy in the spectral domain as a function of spatial position of a seismometer **and can be used to identify cavity position**.

Conclusions (3/3)

- **The potential to identify cavity position is considerably larger for regional/distant sources than for local aftershocks**. This is because the seismic wavefield due to an aftershock is considerably affected or even dominated by the radiation pattern of the source.

- Our simulations and analyses of the seismic noise **indicate possibility to use for identification of cavity position also records of seismic noise.**
  It is, probably, necessary to acquire sufficiently long records of the seismic noise.

Thank you for your attention